ENGINEERING CYANIDE-TOLERANT *ARABIDOPSIS THALIANA*

By EMANG MOLOJWANE

Dissertation presented for the degree of Master of Science

in the Department of Molecular and Cell Biology

University of Cape Town

March 2015

Supervisor: Robert Ingle

PLAGIARISM DECLARATION

I know the meaning of plagiarism and declare that all of the work in the dissertation, save for that which is properly acknowledged, is my own.

I have used the Harvard-UCT (Author-Date) convention for citation and referencing.

……. ……..

Signature: Emang Molojwane Date

ABSTRACT

ENGINEERING CYANIDE-TOLERANT *ARABIDOPSIS THALIANA*

Emang Molojwane, University of Cape Town (March 2015)

Supervisor: Robert Ingle

Cyanide is highly toxic as it inhibits respiration in aerobic organisms by binding to cytochrome *c* oxidase in the mitochondrial electron transport chain. Plants naturally produce cyanide from the hydrolysis of cyanogenic glycosides and as a by-product of ethylene biosynthesis. β-Cyanoalanine synthase prevents self-poisoning by combining endogenous cyanide with cysteine in the mitochondria to form β-cyanoalanine, which is further hydrolysed to asparagine, or aspartate and ammonia, by plant nitrilase 4 enzymes. β-Cyanoalanine synthase activity enables plants to detoxify limited concentrations of exogenous cyanide. However, phytotoxicity and death occur from exposure to relatively low concentrations of exogenous cyanide. In contrast, some microorganisms have a high capacity for cyanide detoxification due to a number of metabolic pathways including the degradation of cyanide to formate and ammonia; or formamide, by bacterial cyanidase (CynD) and fungal cyanide hydratase (CHT), respectively.

Environmental contamination caused by failure to contain cyanide from anthropogenic sources is an important global problem. Hydrometallurgical gold mining utilises cyanide as a lixiviant due to the high affinity of cyanide for gold and the stability of the resulting cyanometallic complexes in aqueous solution, and thus is a significant source of cyanide contamination of soil and water. Biological treatment methods for cyanide, such as phytoremediation, could provide alternatives to the currently used chemical destruction techniques with their associated disadvantages. The use of phytoremediation would require plants to tolerate high concentrations of cyanide in soil. Two attempts have previously been made, with some success, to increase cyanide tolerance in Arabidopsis by genetic engineering: the first, by augmenting the β-cyanoalanine synthase pathway using a microbial nitrilase; and, the second, by introducing a microbial detoxification pathway targeted to the chloroplasts while overexpressing the endogenous enzyme which metabolises the product of the cyanide detoxification reaction. The aim of the current study was to determine whether *Arabidopsis thaliana* could co-opt the *CynD* and *CHT* genes from the cyanide-degrading *Bacillus pumilus* and *Neurospora crassa* to detoxify higher levels of cyanide using the encoded enzymes, and whether targeting CynD and CHT to the mitochondria would confer a greater enhancement of cyanide tolerance on plants compared to targeting to the cytoplasm.

Arabidopsis thaliana plants were genetically engineered to express either *CynD* or *CHT*. Plant lines expressing the same genes targeted to the mitochondria, *atp-CynD* or *atp-CHT* were also established. The integration of transgenes into the genome was confirmed by PCR genotyping and the relative expression of transgenes in homozygous plant lines determined using quantitative PCR. Homozygous transgenic Arabidopsis was then assessed for the ability to grow in the presence of cyanide compared to wild-type Col-0.

Plants were successfully transformed with *CynD*, *CHT*, *atp-CynD* and *atp-CHT*. Although *CynD* was detected in the genome, there was no transcript amplified from the plant cDNA. *CHT* transcript was detected but it was not possible to determine its relative expression. *CynD* and *CHT* plants were excluded from further tests. Col-0, *atp-CynD* and *atp-CHT* seeds were able to germinate in the presence of 50 µM KCN. *atp-CynD* and *atp-CHT* displayed significantly improved root growth in the presence of 50 µM KCN: 75% and 70% relative root growth, respectively, compared to 50% for Col-0. Root lengths of *atp-CynD* and *atp-CHT* plants were 41–54% longer than Col-0 plants in the presence of 50 µM KCN. Thus, it was demonstrated that *Arabidopsis thaliana* could use *Bacillus pumilus* CynD and *Neurospora crassa* CHT pathways to detoxify cyanide. This study provided further evidence for the potential of genetic engineering to increase cyanide tolerance in plants. Even with increased tolerance, transgenic Arabidopsis experienced decreased growth in the presence of cyanide. Therefore, future work could involve generating transgenic plants using a combination of the three genetic engineering strategies attempted thus far to investigate whether simultaneous targeting of heterologous microbial nitrilases to the cytoplasm, chloroplasts and mitochondria would be more effective in increasing cyanide tolerance in plants.

DEDICATION

This thesis is dedicated to my grandmother, Ipo Ntshole, who would have been so proud; my mother and father for their love and support; my sister and brother for running around on my behalf many a time and to Enele, the newest addition to the family, who came into the world under the most trying of circumstances.

ACKNOWLEDGEMENTS

I would like to thank Trevor Sewell for providing bacterial clones of *CynD* and *CHT*; David Logan for the pBIN*mgfp5-atpase* vector; Laura Roden for providing OneShot cells and pFAST-G02 clones; Brendan O'Leary for providing advice on cyanide tolerance assays; Faezah Davids & Madhu Chauhan for their assistance with acquiring and using equipment.

I would like to the MCB Equity Development Program for the EDP bursary and Robert Ingle for a top-up bursary.

I would also like to thank Rob Ingle and the members of Lab 430, past and present, for their assistance, advice and support, and countless other things outside of the laboratory.

TABLE OF CONTENTS

LIST OF FIGURES

LIST OF TABLES

CHAPTER 1: LITERATURE REVIEW

1.1 Chemical properties of cyanide

Cyanide, hereafter CN, refers to a negatively-charged ion consisting of one carbon atom bound to one nitrogen atom by a triple covalent bond, $C{\equiv}N^-$ or CN^-. The cyanide anion and hydrogen cyanide, HCN, are collectively referred to as free cyanide (Zagury, Oudjehani & Deschênes, 2004; Johnson, in press).

CN has a high affinity for metals and reacts with them to form simple and complex cyanides with a wide range of chemical stabilities (Dash, Gaur & Balomajumder, 2009). Simple cyanides include sodium cyanide, NaCN, potassium cyanide, KCN, and calcium cyanide, $Ca(CN)_2$, which are readily soluble and dissociate into CN and HCN (Dash, Gaur & Balomajumder, 2009; Zagury, Oudjehani & Deschênes, 2004). Hydrolysis of CN produces HCN which then dissociates into a hydrogen ion, H^+, and CN (Johnson, in press). Therefore, both CN and HCN are present in solution (Johnson, in press). Formation of the anion is favoured at alkaline pH levels above the pK_a (9.3) of HCN, whereas at acidic pH, HCN formation is favoured (Johnson, in press). HCN may volatilize from aqueous solution because it has a high vapour pressure (Johnson, in press). Simple cyanides also include relatively insoluble compounds such as $Zn(CN)_2$, $Cd(CN)_2$ and CuCN (Dash, Gaur & Balomajumder, 2009; Zagury, Oudjehani & Deschênes, 2004). These are also referred to as weak-acid dissociable cyanide complexes since CN can be liberated from them under moderately acidic conditions (Dash, Gaur & Balomajumder, 2009).

Highly stable complexes of CN can be formed with metals such cobalt, iron, silver and gold (Dash, Gaur & Balomajumder, 2009; Zagury, Oudjehani & Deschênes, 2004). For example, CN reacts with iron to form ferrocyanide ($Fe(CN)_6^{-4}$) and ferricyanide ($Fe(CN)_6^{-3}$) complexes (Ebbs, 2004). These stable complexes will dissociate under extremely acidic conditions and are referred to as strong-acid dissociable cyanides (Zagury, Oudjehani & Deschênes, 2004).

1.2 Molecular and physiological effects of cyanide in plants

Free cyanide is the most toxic of the forms of cyanide (Dash, Gaur & Balomajumder, 2009). Inhibition of aerobic respiration through the irreversible binding of cytochrome *c* oxidase in the mitochondrial electron transport chain is a well-known mechanism by which CN toxicity occurs in living organisms (Wen et al., 1997). The respiratory electron transport chain transfers electrons produced by the oxidation of electron donors such as reduced nicotinamide adenine dinucleotide, NADH, from one

electron carrier to the next, through a series of redox reactions. In the final step of this process, cytochrome *c* oxidase transfers electrons to oxygen which is thus reduced to form water within the mitochondrial matrix. The energy released during the transfer of electrons down the electron transport chain is used to establish a proton gradient across the membrane which then provides the energy that drives the synthesis of the energy carrier molecule, adenosine triphosphate, ATP, from adenosine diphosphate and inorganic phosphate, by ATP synthase. Binding of the haem iron in the terminal oxidase by CN prevents the electron transfer to oxygen (Way, 1984). Thus, oxidative phosphorylation is inhibited and the affected tissues become energy-deficient due to the associated lack of ATP synthesis. Plants have the ability to bypass the cytochrome *c* oxidase and instead deliver electrons to oxygen via an alternative terminal oxidase thus enabling some form of CN-resistant respiration (Elthon, Nickels & McIntosh, 1989).

CN also inhibits other (metallo)enzymes involving Schiff base intermediates (Way, 1984). For example, CN inhibits the activity of ribulose-1,5-diphosphate carboxylase (Rubisco) which catalyses the initial carbon dioxide, CO_2, fixation in the Calvin cycle (Wishnick & Lane, 1969). CN binds to the enzyme while it is bound to ribulose-1,5-diphosphate, forming an inactive complex composed of Rubisco, ribulose-1,5-diphosphate and CN in a ratio of 1:1:1 (Wishnick & Lane, 1969). CN has been shown to inhibit both photosynthesis and catalase activity in intact chloroplast preparations (Allen & Whatley, 1978; Forti & Gerola, 1977). Forti and Gerola (1977) proposed that hydrogen peroxide accumulation was responsible for inhibition of the carbon cycle enzymes. Allen and Whatley (1978) found it more plausible that inhibition of Rubisco (and therefore the rest of the Calvin cycle) by CN resulted in a lack of oxidised nicotinamide adenine dinucleotide phosphate, NADP, to serve as an electron acceptor for photosystem I, causing the substitution of oxygen for NADP and leading to hydrogen peroxide accumulation in the absence of active catalase.

The physiological effects of CN are dependent on the concentration present. Exposure to toxic concentrations of CN causes a reduction in plant biomass accumulation. Plants growing in the presence of high levels of CN have a smaller size and lower mass than those growing in the absence of CN (McMahon Smith & Arteca, 2000). Root growth is reduced or stopped in the presence of CN (O'Leary, Preston & Sweetlove, 2014; Akcil, 2003; Alström & Burns, 1989). The root growth of pre-germinated lettuce (*Lactuca sativa*) seeds was completely inhibited by 80 nmol mL^{-1} KCN in the growth agar after four days (Alström & Burns, 1989). In fact, the inhibition of plant growth by some growth-inhibitory rhizobacteria, for example, *Pseudomonas fluorescens* strain S241, may be partly attributable to the presence of CN in the volatile compounds produced by such organisms when CN

is produced in sufficiently high amounts in soil (Alström & Burns, 1989). *Arabidopsis thaliana* exposed for three weeks to volatile compounds produced by *Pseudomonas*, *Chromobacterium* and *Serratia* bacterial strains had reduced fresh weight, relative to untreated control plants, in response to increasing total HCN although the effect was more pronounced when the same concentration was supplied as chemical HCN compared to bacterial volatile HCN (Blom et al., 2011).

Another symptom of CN toxicity is the bleaching of leaves as a result of a decrease in the rate of chlorophyll production and accumulation as observed in *A. thaliana* exposed to 50 µM HCN (McMahon Smith & Arteca, 2000). Reduced transpiration is another indicator of CN phytotoxicity and can lead to wilting. Exposure to KCN amounting to 2 mg CN L^{-1} in nutrient solution reduced the transpiration rate of basket willows (*Salix viminalis*) by more than 50% after 72 h (Larsen, Trapp & Pirandello, 2004). Ultimately the accumulation of CN within plant tissues is lethal. Basket willows exposed to 2 mg CN L^{-1} died within three weeks and those exposed to 8 and 20 mg CN L^{-1} died within a week (Larsen, Trapp & Pirandello, 2004).

Conversely, CN in non-toxic amounts can stimulate growth in plants. A growth stimulatory effect was detected in weeping willow (*Salix babylonica*) in response to CN supplied as KCN in hydroponic growth medium (Yu, Gu & Liu, 2007). After 192 h of exposure, the transpiration rate of the willows was significantly higher than the control plants at concentrations of 2.37 mg CN L^{-1} and higher. At concentrations of 1.19 mg CN L^{-1} and 4.74 mg CN L^{-1}, respectively, chlorophyll production and soluble protein reached their maximum at levels that were significantly greater than in untreated plants. Seedlings of pigweed (*Amaranthus albus*), lettuce (*Lactuca sativa*) and pepperweed (*Lepidium virginicum*) that were germinated in the presence of 0.1–1.0 mM KCN were larger than untreated seedlings (Taylorson & Hendricks, 1973).

Seed exposure to CN can promote germination and break seed dormancy in some species. CN applied as HCN gas to sunflower (*Helianthus annuus*) embryos without pericarps reduced their dormancy (Oracz et al., 2009). CN vapours produced by up to 1 mM KCN were able to break the dormancy of *Arabidopsis thaliana* ecotype C-24 seeds. CN vapours formed through the photolysis of sodium nitroprusside, potassium ferrocyanide (Fe(II)CN) and potassium ferricyanide (Fe(III)CN) were also shown to reduce *A. thaliana* C-24 seed dormancy (Bethke et al., 2006; Bethke, Libourel & Jones, 2006). CN is released from the hydrolysis of glyceronitrile, a cyanohydrin formed during the burning of plant matter (Flematti et al., 2011). Cyanohydrins are organic compounds containing both a CN and hydroxyl (OH) functional group attached to the same carbon atom. In fire-prone environments,

when water is present, CN released from glyceronitrile promotes seed germination in a variety of plant species thus enabling the establishment of new vegetation following a fire (Flematti et al., 2011). The mechanism by which CN reduces dormancy has not been conclusively elucidated. It has been suggested that dormancy is alleviated as a result of increased intracellular nitric oxide (Bethke, Libourel & Jones, 2006) and increased reactive oxygen species, which may play a role in producing the effects which have been attributed to nitric oxide in experiments using sodium nitroprusside (Oracz et al., 2009), in response to CN.

Under nitrogen-limiting conditions, plants can use CN as a source of nitrogen such that the proportion of nitrogen derived from CN is increased whilst the total nitrogen content of the tissue remains the same (Ebbs et al., 2010). When wheat (*Triticum aestivum*) and sorghum (*Sorghum bicolor*) were exposed to 5–200 µM $KC^{15}N$ in the presence of sufficient nitrogen in the hydroponic growth medium, there was no difference in the enrichment of radioactively-labelled nitrogen from CN within the plant tissues across the different concentrations (Ebbs et al., 2010). However, in the absence of inorganic nitrogen, the ^{15}N enrichment within sorghum plants exposed to 50, 100 and 200 µM $KC^{15}N$ was significantly increased (Ebbs et al., 2010). In wheat, the enrichment was significantly greater only at 200 µM and only in the roots, unlike sorghum, which showed no differences between the roots and shoots. For each plant type, total tissue nitrogen remained the same across the different treatments and within a tissue (Ebbs et al., 2010). The plants showed a preference for ammonium over CN as a nitrogen source when the two were available concurrently. When wheat plants were exposed to 100 µM KCN in the presence of ammonium (up to 100 µM) and a fixed concentration of nitrate, the enrichment from KCN nitrogen was decreased significantly (Ebbs et al., 2010).

1.3 Cyanide generation by plants and other organisms

CN occurs in the natural environment as a product of cyanogenesis by organisms such as algae, bacteria, fungi and plants. In bacteria and fungi, HCN is a metabolic by-product and is not known to have a specific physiological function. Bacterial CN is produced by the oxidative decarboxylation of glycine which is catalysed by HCN synthase, an enzyme that is most likely an amino acid dehydrogenase (Blumer & Haas, 2000). HCN is derived from the methylene carbon of glycine without breaking of the C-N bond, and CO_2 from the carboxyl group (Blumer & Haas, 2000; Knowles, 1976). The maximal rate and amount of HCN is produced in the early stationary growth phase (Blumer & Haas, 2000; Knowles, 1976).

Bacterial cyanogenesis is known to occur in fluorescent pseudomonads, the proteobacteria *Chromobacterium violaceum*, some cyanobacteria (e.g. *Anacystis nidulans*) and *Rhizobium leguminosarum* (Blom et al., 2011; Blumer & Haas, 2000; Alström & Burns, 1989). HCN from *Pseudomonas fluorescens* CHA0 has been shown under laboratory conditions to inhibit the cytochrome *c* oxidase of a termite (*Odontotermes obesus*) pest in the laboratory in a manner similar to the effect of KCN on the termite cytochrome *c* oxidase activity and causes termite mortality (Devi & Kothamasi, 2009). Two hours of termite exposure to a 24 h culture of *P. fluorescens* CHA0 which produced approximately 20 µM HCN caused 100% mortality of termites. Exposure to the non-cyanogenic *P. fluorescens* resulted in 30% mortality due to factors other than HCN but did not cause any change in cytochrome *c* oxidase activity compared to unexposed termites (Devi & Kothamasi, 2009). A wide range of fungal genera produce CN (Knowles, 1976). Fungal HCN can have antibiotic effects against other fungi and bacteria, and have inhibitory effects on germination and seedling growth of specific plants (Knowles, 1976).

The main sources of CN production in plants are the hydrolysis of cyanogenic glycosides, CGs, and as a by-product of metabolic pathways. CGs are molecules consisting of a sugar moiety covalently bound to an α-hydroxynitrile (cyanohydrin); they are *O*-β-glycosidic derivatives of α-hydroxynitriles (Zagrobelny et al., 2004; Poulton, 1990; Knowles, 1976). The sugar in most CGs is glucose (Vetter, 2000). α-Hydroxynitriles are formed from amino acids through a series of steps (Zagrobelny et al., 2004) and are subsequently glycosylated by soluble *O*-glycosyltransferases to the final CGs (Poulton, 1990). The majority of CGs is derived from the proteinogenic amino acids tyrosine, phenylalanine, valine, leucine and isoleucine (Zagrobelny et al., 2004; Poulton, 1990). Examples of CGs derived from these amino acids include lotaustralin derived from isoleucine, amygdalin and prunasin from phenylalanine, dhurrin from tyrosine, and linamarin from valine (Knowles, 1976). Thus the aliphatic, aromatic or cyclopentenoid nature of the CG is determined by the amino acid from which it is derived (Poulton, 1990). The non-proteinogenic amino acid cyclopentenyl-glycine is a precursor for cyclopentenoid CGs (Zagrobelny et al., 2004; Poulton, 1990).

At least 75 types of CGs exist in more than 3000 plant species across 110 families of ferns, gymnosperms and angiosperms (Poulton, 1990). Interestingly, a significantly higher proportion of plants that serve as food for humans is cyanogenic, compared to other non-food plants (Jones, 1998). Examples of the former are *Prunus dulcis* (almond), *Manihot esculenta* (cassava), *Phaseolus lunatus* (lima bean), *S. bicolor* (sorghum), and *Colocasia esculenta* (taro) (Jones, 1998; Miller & Conn, 1980). Bitter almonds, cassava root, lima beans and sorghum have been shown to produce 250, 53,

10–312, and 250 mg HCN 100 g^{-1} from the CGs amygdalin, linamarin, linamarin and dhurrin, respectively (Fokunang et al., 2001). HCN potential may vary according to tissue e.g. cassava root tubers can contain 240–890 mg kg^{-1} CGs compared to 1040 mg kg^{-1} in leaves (Jones, 1998). Most food plants are cyanogenic in tissues that are not generally eaten such as leaves. Some foods, however, are the cyanogenic part of the plant and therefore the removal of CN during pre-ingestion processing is vital to make them safe for human consumption. For example, CGs and HCN can be reduced to safe levels in cassava by chopping and grinding in running water (Fokunang et al., 2001).

A major function of CGs is chemical defence of the plant against feeding by herbivores including insects (Zagrobelny et al., 2004). This cyanogenic defence has been documented in sorghum against locusts (*Locusta migratoria*), for example (Jones, 1998). CGs in intact plants are generally sequestered away from the endogenous hydrolytic enzymes that degrade them (Poulton, 1990). β-Glucosidases catalyse the removal of the sugar moiety to leave the corresponding α-hydroxynitrile which is then further degraded to HCN and a ketone or aldehyde by hydroxynitrile lyase (Zagrobelny et al., 2004; Poulton, 1990). An analysis of protoplast extracts from *S. bicolor* leaf blades revealed that dhurrin was almost exclusively located in the vacuoles of epidermal cells, and the dhurrin β-glucosidase (dhurrinase) and hydroxynitrile lyase were found almost exclusively in the mesophyllic cells (Kojima et al., 1979). Dhurrinase was found to be located in the chloroplasts, whereas the hydroxynitrile lyase was cytoplasmic (Thayer & Conn, 1981). In other species, the CG and enzymes may be located in different compartments of the same cells (Poulton, 1990). In either case, the disruption of plant tissues, such as that caused by chewing, results in mixing of the CGs and enzymes leading to the release of HCN. The degradation of the α-hydroxynitrile may occur spontaneously at above pH 5.5–6 or by the aforementioned enzymatic activity of hydroxynitrile lyase at pHs below 5.5 (Zagrobelny et al., 2004; Poulton, 1990).

In plants that do not accumulate CGs, the major source of endogenous CN is that produced as a metabolic by-product. The most significant metabolic pathway by which CN is produced is the biosynthesis of ethylene, a hormone that is produced in all plants and plays a role in many processes throughout the different developmental stages, e.g. germination of seeds, leaf senescence and ripening of fruit (Romero et al., 2014; Yip & Yang, 1988; Peiser et al., 1984). Ethylene is formed from the oxidation of 1-aminocyclopropane-1-carboxylic acid (ACC) (Yip & Yang, 1988) which is catalysed by ACC oxidase (John, 1997). This reaction produces ethylene and a cyanoformate ion which subsequently spontaneously degrades into CN and CO_2 (Murphy et al., 2014; Peiser et al., 1984). A molecule of HCN is produced for every molecule of ethylene synthesised (Peiser et al., 1984). CN is

also produced in plants during periods of stress, presumably as a result of increased ethylene synthesis in response to the stress (Liang, 2003). One day of drought stress, resulting in a 28% decrease in relative water content caused an increase in endogenous CN from 92.2 nmol g^{-1} to 673.2 nmol g^{-1} dry weight in tobacco (*Nicotiana tabacum*) plants (Liang, 2003).

1.4 Biochemical degradation of cyanide in plants

Steady-state endogenous CN levels in healthy plants have no deleterious effects, meaning that there is no accumulation of toxic concentrations of CN within tissues. As the physiological pH is lower than the pK_a of HCN (9.3) the bulk of CN contained in plant tissues is in the form of HCN (Yip & Yang, 1988). A ubiquitous two-step detoxification mechanism is the primary means by which HCN toxicity is prevented in plants. The first step takes place in the mitochondria, a major site of CN toxicity, where HCN is combined with cysteine to produce the non-proteinogenic amino acid β-cyanoalanine and hydrogen sulphide (Figure 1) in a reaction catalysed by β-cyanoalanine synthase (CAS) (Hatzfeld et al., 2000; Blumenthal et al., 1968). CAS is highly specific for cysteine and a different three-carbon amino acid such as serine cannot serve as an alternative substrate (Blumenthal et al., 1968).

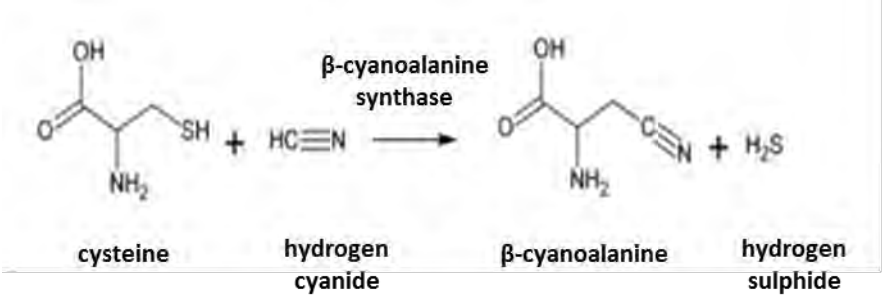

Figure 1: The first step of the β-cyanoalanine synthase cyanide detoxification pathway. β-Cyanoalanine synthase combines free cyanide with cysteine to form β-cyanoalanine (adapted from Budde & Roth, 2011).

CAS also exhibits low-level cysteine synthase (*O*-acetylserine(thiol)lyase) activity (Hatzfeld et al., 2000). Cysteine synthase belongs to the same enzyme family within the superfamily of pyridoxal-5'-phosphate-dependent enzymes as CAS, that is, the β-substituted alanine synthases, and catalyses the addition of hydrogen sulphide to *O*-acetylserine to form cysteine (Watanabe et al., 2008; Hatzfeld et al., 2000). The CAS enzyme from spinach (*Spinacia oleracea*) was shown to have 382-fold higher CAS activity compared to cysteine synthase activity in crude protein extracts from recombinant *Escherichia coli* (Hatzfeld et al., 2000). Similarly, the CAS from *A. thaliana*, encoded by *AtCysC1*, had CAS activity that was 168-fold higher than its cysteine synthase activity (Hatzfeld et al., 2000). However, since *AtcysC1* mutants displayed no significant reduction in cysteine synthase

activity compared to wild-type Col-0 plants, it is unlikely that CAS performs a major role in cysteine biosynthesis *in vivo* (Watanabe et al., 2008).

On the other hand, the CAS activity of a cytosolic cysteine synthase does appear to contribute to the detoxification of CN (Watanabe et al., 2008). Knockout of the gene encoding this enzyme in Arabidopsis (*AtcysA1*) resulted in significantly reduced CAS activity albeit to a lesser extent than in *AtcysC1* mutants (Watanabe et al., 2008). However, even though the residual CAS activity measured in protein extracts from plant tissues of knockout mutants for either gene was insufficient to maintain wild-type CAS activity levels in Arabidopsis (Watanabe et al., 2008), the two enzymes were found to be functionally redundant in CN tolerance (Machingura & Ebbs, 2014). Single *AtcysA1* and *AtcysC1* mutants did not suffer deleterious effects on fresh weight, chlorophyll content, transpiration and relative water content of shoots in response to a seven- to ten-day exposure to 2.5–30 mg CN L^{-1} at a greater rate than wild-type plants (Machingura & Ebbs, 2014).

Hydrogen sulphide, produced during the formation of β-cyanoalanine, inhibits cytochrome *c* oxidase thus inhibiting aerobic respiration (Birke et al., 2012). Mitochondrial cysteine synthase C (OAS-C) detoxifies sulphide through cysteine synthesis (Birke et al., 2012; Romero et al., 2014). In this way, OAS-C plays a supporting role but is not a pre-requisite for CN detoxification (Birke et al., 2012).

The second step of the CN detoxification process involves the hydrolysis of the β-cyanoalanine intermediate. β-Cyanoalanine is a nitrile, that is, an organic compound containing a C≡N group. Nitrilases are enzymes that hydrolyse nitriles to the corresponding carboxylic acid and ammonia (Figure 2). Nitrile hydratases convert nitriles to the corresponding amide (Piotrowski, Schönfelder & Weiler, 2001). The higher plant nitrilases were first characterized in *A. thaliana* and found to fall into two groups (Piotrowski, Schönfelder & Weiler, 2001). The first consists of nitrilases 1, 2 and 3, and the second group consists of nitrilase 4 (NIT4) enzymes. *AtNIT4* homologues are common throughout the plant kingdom, possess both nitrilase and nitrile hydratase activities and specifically hydrolyse β-cyanoalanine (Piotrowski, Schönfelder & Weiler, 2001). During CN detoxification, NIT4 hydrolyses β-cyanoalanine to asparagine, or aspartic acid and ammonia (Figure 2) (Piotrowski & Volmer, 2006). During the former reaction, the C and N atoms from HCN are incorporated into the amide group of asparagine (Blumenthal et al., 1968). The ratio of nitrile hydratase:nitrilase activity of NIT4 varies according to species (Piotrowski & Volmer, 2006; Piotrowski, Schönfelder & Weiler, 2001). *Atnit4* mutants had a heightened sensitivity to exogenously applied CN and β-cyanoalanine, experiencing decreased fresh weight and chlorophyll production, followed by permanent wilting

after a seven-day exposure to 30 mg CN L^{-1}. They also had 50% mortality in the presence of 1.3–13 mg β-cyanoalanine L^{-1} concentrations which had no lethal effect on wild-type or CAS activity mutants (Machingura & Ebbs, 2014).

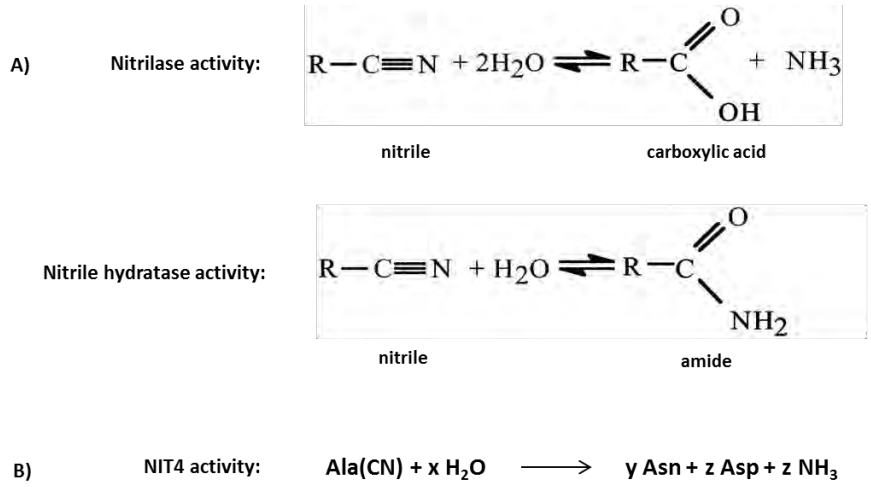

Figure 2: Reactions catalysed by nitrilase and nitrile hydratase enzymes and the second step of the β-cyanoalanine synthase cyanide detoxification pathway. Nitrilase 4 (NIT4) possesses both nitrile hydratase and nitrilase activities (A) which convert β-cyanoalanine (Ala[CN]) into asparagine (Asn) or aspartic acid (Asp) and ammonia (B), respectively, in a ratio which is dependent on the plant species (adapted from Piotrowski & Volmer, 2006; Jandhyala et al., 2005).

In a few species, such as *Vicia sativa* (common vetch), instead of asparagine formation, CN detoxification instead terminates in the conversion of β-cyanoalanine to the dipeptide γ-glutamyl-β-cyanoalanine by γ-glutamyltransferase (Peiser et al., 1984). Arabidopsis has also been shown to produce γ-glutamyl-β-cyanoalanine in addition to asparagine and aspartate (Watanabe et al., 2008).

CN may also be detoxified by conversion to thiocyanate (SCN) catalysed by rhodanese, a much less common pathway in plants, or mercaptopyruvate sulphurtransferase (Figure 3) (García et al., 2010; Watanabe et al., 2008; Miller & Conn, 1980). The significance of the contribution of sulphurtransferases to CN detoxification is yet to be established (Meyer et al., 2003).

The activity of CAS and NIT4 is generally considered sufficient to detoxify endogenous CN generated in plants. Yip and Yang (1988) found that while the ethylene synthesis rate more than doubled when apple slices were supplied with exogenous ACC, there was no detectable HCN gas accumulation and the tissue CN did not exceed the levels present in untreated apple slices. Similarly, a 1000-fold increase in ethylene production resulted in only a doubling of CAS activity in avocado fruit at the

climacteric stage of ripening, supporting their contention that basal CAS activity is high and sufficient to detoxify ethylene synthesis-generated HCN (Yip & Yang, 1988). However, others such as Wen et al. (1997) have reported a correlation between ethylene biosynthesis and CAS activity; the evolution of HCN increased along with ethylene synthesis during ageing of potato (*Solanum tuberosum*) slices and this increase was accompanied by an increase in CAS activity.

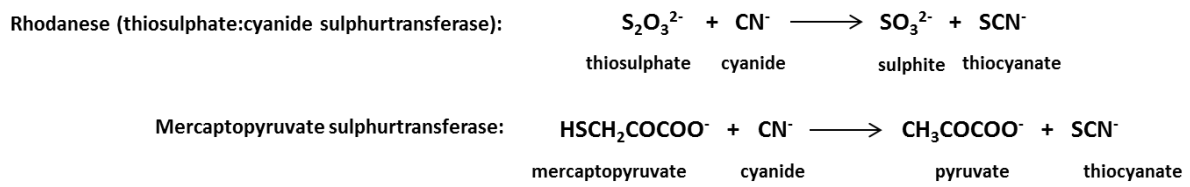

Figure 3: Detoxification of cyanide by conversion to thiocyanate catalysed by rhodanese and mercaptopyruvate sulphurtransferase (adapted from Nakamura, Yamaguchi & Sano, 2000).

Ethylene itself can directly modulate CAS enzyme activity. For example, CAS activity has been shown to increase with exposure to increasing concentrations of ethylene (0–100 µL L^{-1}) and increasing duration of exposure to a constant ethylene concentration (1 µL L^{-1}) in pea (*Pisum sativum*) seedlings and six other species including barley (*Hordeum vulgare*) and bread wheat (*Triticum aestivum*) (Goudey, Tittle & Spencer, 1989). In contrast, CAS activity in Arabidopsis decreased in response to 1 µL L^{-1} ethylene exposure for up to 24 h (Meyer et al., 2003).

CAS activity can also be modulated by exogenous CN concentrations in some species. In response to exogenous KCN, CAS activity increased significantly in the roots and shoots of rice (*Oryza sativa*) seedlings and the rate at which KCN was metabolised following uptake was more rapid in seedlings exposed to higher KCN concentrations (the rate of metabolism of 2.04 mg CN L^{-1} was more than five-fold higher than that of 0.45 mg CN L^{-1} (Yu, Lu & Yu, 2012). Only small percentages (1.6–5.68%) of the CN lost from the aqueous KCN solution were recovered in the total CN content of plant tissues (roots and shoots) and there was no significant difference between total CN content in plants exposed to different concentrations of KCN (Yu, Lu & Yu, 2012) indicating that the CN was effectively metabolised. The decrease in solution CN was not due to loss of HCN by volatilisation because there was no measurable change in the CN concentration in the control KCN solution without rice seedlings over the exposure period (48 h) (Yu, Lu & Yu, 2012). In tobacco, intermittent spraying of leaves with 10 µM KCN caused a modest increase in CAS activity within 24 h (Liang, 2003). However, in Arabidopsis, exposure to 30 mg CN L^{-1} in nutrient solution for up to 36 h and spraying of leaves with 20 mM CN did not significantly alter CAS activity in wild-type plants (Machingura & Ebbs, 2014). The increase in CN uptake by plants under conditions of nitrogen deficiency is accompanied by an

increase in CAS activity. Wheat exposed to 100 µM KCN in nitrogen-deficient nutrient solution had significantly higher CAS activity, more so in roots than in shoots, than plants in nutrient solution replete with inorganic nitrogen (Machingura & Ebbs, 2010).

The critical exogenous CN concentration at which the detoxification capacity of the CAS pathway is overwhelmed varies according to factors such as plant species, whether the CN is applied in soil or solution, and temperature (see section 1.6). It may also be linked to whether plants are cyanogenic or acyanogenic although this has not been conclusively shown (Yu et al., 2004; Miller & Conn, 1980).

1.5 Biochemical mechanisms of cyanide degradation in microorganisms

The CN-degrading capacity of certain bacteria and fungi exceeds that of plants. For example, a strain of *Bacillus pumilus* that was isolated from a slimes dam at a South African gold mine could deplete the CN content of a 100 mg CN L^{-1} solution (Meyers et al., 1991). Elsewhere, a *B. pumilus* strain was isolated that could grow in media containing 2600 mg CN L^{-1} (0.1 M KCN) and survive in up to 2.5 M KCN solution (Skowronski & Strobel, 1969). Microorganisms with particularly high degradative capacities have been identified, such as *Alcaligenes xylosoxidans* subsp. *denitrificans* strain DF3, which could degrade 26,190 mg HCN L^{-1} to less than ≈0.002 mg HCN L^{-1} in 55 h (Ingvorsen, Højer-Pedersen & Godtfredsen, 1991).

Nitrilase, nitrile hydratase, cyanide hydratase (CHT) and cyanide dihydratase or cyanidase (CynD) enzymes catalyse the hydrolytic degradation of CN in microorganisms (Ebbs, 2004). As in plants, nitrilase and nitrile hydratase enzymes convert nitriles into the corresponding carboxylic acid and amide, respectively (Ebbs, 2004). CHT is mainly a fungal enzyme and it converts HCN into formamide (Ebbs, 2004). Recombinant CHT from *Neurospora crassa* has been shown to be relatively stable to pH and temperature over the ranges pH 5–9 and 37–43°C (Basile et al., 2008). Cyanide dihydratase is mainly a bacterial enzyme and converts HCN into formate and ammonia (Ebbs, 2004; Meyers et al., 1993). *A. xylosoxidans* subsp. *denitrificans* degrades CN using the CynD pathway (Ingvorsen, Højer-Pedersen & Godtfredsen, 1991). Purified recombinant CynD from *B. pumilus* was shown to be stable over the temperature range 23–42°C and to have maximum activity between pH 7 and 8 (Jandhyala et al., 2005). CHT and CynD have high specificities for HCN compared to nitrilases and nitrile hydratases which have a range of substrates (Ebbs, 2004; Meyers et al., 1993).

Other CN degradation pathways involve oxidation, reduction, and substitution/transfer mechanisms (Ebbs, 2004). Oxidative reaction pathways are catalysed by cyanide monoxygenase and cyanide

dioxygenase (Ebbs, 2004). Cyanide dioxygenase converts HCN to CO_2 and ammonia directly, whereas cyanide monoxygenase converts CN to cyanate (OCN), which is further combined with bicarbonate by cyanase to form ammonia and CO_2 (Ebbs, 2004). Cyanase is a catalyst for one of two SCN degradation pathways, converting SCN to OCN which is then converted to ammonia and CO_2 as previously described (Ebbs, 2004). An example of a transfer reaction is the combination of CN with thiosulphate to form SCN, catalysed by thiosulphate:cyanide sulphurtransferase or rhodanese (Figure 3) (Ebbs, 2004).

Some organisms detoxify CN using multiple pathways, the use of which is determined by external factors such as CN concentration, oxygen and pH (Ebbs, 2004). In a manner similar to plants, microbial growth and CN metabolism are reduced when microbes are exposed to a CN concentration which is higher than an organism-specific threshold (Ebbs, 2004).

1.6 Environmental contamination with cyanide and the potential for phytoremediation

Due to the large amounts of anthropogenic CN that are introduced into the environment annually, plants are liable to encounter toxic levels of CN. HCN is widely used in industry and approximately 1.1 million t of HCN is produced globally every year. Industries such as computer electronics, pharmaceuticals, adhesives and nylon manufacturing use CN (Mudder & Botz, 2004). In Europe and the USA, manufactured gas plants generated significant amounts of CN waste during the 19th and 20th century. This waste persists in the old sites today in the form of exhausted purifier beds, previously used to scrub the CN and hydrogen sulphide by-products of the gas production, and subsequently disposed of on-site as fill material (Kang et al., 2008). CN (mostly iron cyanide complexes which release free CN upon photolysis by ultraviolet, UV, light) contaminates the surrounding soil and poses challenges for the development of these sites as well as the risk of environmental pollution (Kang et al., 2008).

Currently, gold mining is the primary source of industrial CN waste released into the environment. This is due to the use of cyanidation technology, first used commercially in New Zealand in the late 1800s, which exploits the ability of CN to form strong complexes with metals, thereby enabling the recovery of more gold per kilogram of low grade ore than previously used methods (Korte, Spiteller & Coulston, 2000). Some 90% of the major gold producers in the world use CN in their operations (Mudder & Botz, 2004).

In heap leach mining operations, dilute NaCN solution is sprayed onto the surface of heaps of finely ground gold ore for several months as a lixiviant (Eisler & Wiemeyer, 2004). Each heap is set on an impermeable base on the surface of the ground and can be as large as 1–25 million t and 100 m high, and occupy several hundred hectares (Eisler & Wiemeyer, 2004). The CN forms strong water-soluble complexes with gold as it percolates through the heap. Gold is then chemically recovered from these negatively-charged complexes contained in the effluent solution drained from the base of the heap, leaving behind free CN anion in the waste streams or tailings (Eisler & Wiemeyer, 2004). In a single year, for example, a Turkish gold mine used 125 t of NaCN in 365 000 m^3 of water to leach 750 kg gold from 250 000 t of rock, containing 3 g gold per tonne (Korte, Spiteller & Coulston, 2000). Untreated leftover NaCN solution was stored in open ponds (Korte, Spiteller & Coulston, 2000).

Open air tailings (ore waste) pose a risk to the environment even after the mine is no longer operational because of the risk of escape into the wider environment, possible pollution of groundwater and via dust containing CN, and formation of complexes with metals which persist. Failure to contain CN due to tears or punctures in the pad liners, leaks in liners carrying solution and overflow of open ponds and piles can cause the release of CN into the environment (Eisler & Wiemeyer, 2004). There have been several documented cases of wildlife being adversely affected when CN escaped into the environment as well as relatively infrequent cases resulting in human deaths. Past failures of dams at gold mines in the Philippines, South Africa and Zimbabwe, for example, led to the release of 50 000 m^3, 600 000 m^3 and 30 000 t of CN-contaminated waste causing human fatalities amounting to 12, 17 and 1, respectively (Mudder & Botz, 2004). More recently, in Romania, 100 000 m^3 of CN waste contaminated the drinking water of more than two million people in neighbouring Hungary when it overflowed from a burst dam due to heavy precipitation (Mudder & Botz, 2004; Korte, Spiteller & Coulston, 2000). Therefore, the continued occurrence of unintentional discharges into the environment has meant that the destruction of CN in waste remains a top priority.

Gold mine CN-containing waste is most commonly treated using chemical and physical methods (Akcil, 2003). Destruction of CN is performed using chemical methods such as the INCO sulphur dioxide/air process and hydrogen peroxide treatment which generally involve the oxidation of CN to a less toxic product, OCN, in these specific examples (Akcil, 2003). Both of these processes require a copper catalyst and the former also produces sulphate. Another treatment, alkaline chlorination, converts CN to cyanogen chloride which is then hydrolysed to release OCN and chloride (Akcil, 2003). This treatment can be extended to breakpoint chlorination (Akcil, 2003). While chemical

destruction methods are effective, they can lead to the production of other compounds that are undesirable. OCN hydrolysis may generate potentially toxic ammonia (Akcil, 2003) and chlorination can cause an increase in the total solids present in water (Dash, Gaur & Balomajumder, 2009).

Consequently, as an alternative, biological treatment methods for CN waste have been considered including phytoremediation, that is, the use of plants to clean the environment of pollutants (Pilon-Smits, 2005). Phytoremediation is an environmentally friendly technology which relies on biological processes that are driven by solar energy (Pilon-Smits, 2005). Plants serve as relatively easily managed bioreactors (Larsen, Trapp & Pirandello, 2004). Using plants to clean up CN from contaminated soil is considered an attractive potential option because it is natural, cheaper than chemical methods and offers other plant-associated benefits such as stabilisation of the soil (Pilon-Smits, 2005; Larsen, Trapp & Pirandello, 2004; Nelson, Kroegef & Arps, 1998).

Any plants that might be used for the phytoremediation of CN-contaminated soil must necessarily be able to grow in the presence of CN. Accordingly, a number of plant species have been evaluated for their ability to tolerate CN in growth media and it has been shown that some species have a higher capacity than others to grow in the presence of CN (Larsen, Trapp & Pirandello, 2004; Yu et al., 2004; Trapp et al., 2003). For example, *S. bicolor* irrigated daily for 60 days with water containing 20 or 50 mg CN L^{-1} was able to grow well outdoors in soil, attaining gains in height that were about the same or slightly better than control plants, although the root mass was decreased in the presence of CN (Trapp et al., 2003). Similarly, plants grown indoors in sealed vessels containing soil and watered with CN solution showed slightly better growth and increased transpiration in plants exposed to 50 mg CN L^{-1} compared to untreated plants (Trapp et al., 2003). A comparison of the CN-metabolising activity of the detached leaves of 28 species of Chinese plants from 23 families revealed that a wide range of plants could efficiently metabolise ≈1 mg CN L^{-1}, the best of which was Chinese elder (*Sambucus chinensis*) with a removal capacity of 8.77 mg CN kg^{-1} h^{-1} (Yu et al., 2004).

Plants can be effective at removing a fixed amount of CN from solution. CN concentration was reduced from 0.4, 2, and 8 mg CN L^{-1} to below the detection limit of 0.04 mg CN L^{-1}, and from 20 mg CN L^{-1} to 0.04 mg CN L^{-1} by basket willows by the end of 192 h (Larsen, Trapp & Pirandello, 2004). Control tests indicated that the majority of CN loss was not due to volatilization of HCN either from soil or from leaves following uptake (Trapp et al., 2003). CN removal capacity varies according to species. In sealed vessels, the detached leaves of willow hybrid (*S. viminalis x schwerinii*), black elder (*Sambucus nigra*) and poplar (*Populus robusta*) depleted 90%, 84% and 50%, respectively, of the CN

in a 1 mg CN L^{-1} solution after 18 h (Larsen, Trapp & Pirandello, 2004). Roots of willow, birch (*Betula pendula*), black elder, and poplar were also efficient at removing CN from 1.2 and 6 mg CN L^{-1} solutions within 24–96 h (Larsen, Trapp & Pirandello, 2004). The amount of time required to remove CN from solution became extended in response to increasing starting CN concentration and increasing toxicity. Willow hybrid removed 95% CN from 2 mg CN L^{-1} in 48 h and 82% from 10 mg CN L^{-1} by the end of 168 h, with very little change in the solution CN in the period between 96 and 168 h (Larsen, Trapp & Pirandello, 2004).

Following uptake, non-toxic amounts of CN are metabolised, leaving tissue CN at pre-treatment levels. Basket willows exposed to 0.4 mg CN L^{-1} gave CN readings in treatment solution and plant tissue that were not different from those from the control untreated plants (Larsen, Trapp & Pirandello, 2004). Elevated CN was detected in the roots; roots and leaves; and roots, leaves and stems of plants exposed to 2, 8 and 20 mg CN L^{-1}, respectively, showing that the tissue distribution of accumulated CN increased in the presence of higher CN concentrations (Larsen, Trapp & Pirandello, 2004). In plants with elevated CN, both complexed and easily liberatable, that is, free and simple, CN were found in the tissues even though only free CN was applied (complexation with metal ions within tissues must have occurred); easily liberatable was greater than complexed CN in every case (Larsen, Trapp & Pirandello, 2004). Eventually, these plants died, with those exposed to higher CN concentrations dying more rapidly (Larsen, Trapp & Pirandello, 2004).

An important factor affecting the ability of plants to detoxify exogenous CN is the dose, or the amount taken up into cells per unit of time, which appears to be more important than the absolute concentrations of solutions (Larsen, Trapp & Pirandello, 2004; Trapp et al., 2003). The same concentration of CN can be more or less detrimental depending on how it is administered to plants. Willow hybrids (*S. viminalis x schwerinii*) were exposed to 20 mg CN L^{-1} which was toxic in growth solution but, like sorghum, plants irrigated with this concentration of KCN were able to survive the treatment while growing on sand for 423.5 h albeit with reduced transpiration, displaying no obvious growth effects for 40 days after the application of CN ceased (Larsen, Trapp & Pirandello, 2004). Plants watered with 50 mg CN L^{-1} died at a rate similar to plants grown in 20 mg CN L^{-1} solution (Larsen, Trapp & Pirandello, 2004). This was presumably due a higher dose of CN being taken up from aqueous solution than from soil watered with the same concentration of CN allowing less time for CAS detoxification to work (Larsen, Trapp & Pirandello, 2004; Trapp et al., 2003). Dose-dependent CN toxicity potentially means that high CN concentrations could be cleaned up by plants if administered to the roots at the appropriate rate (Trapp et al. 2003).

Temperature has also been shown to affect the rate of CN metabolism by detached leaves of weeping willow and Chinese elder (Yu et al., 2005). Increasing the temperature (11–32°C) increased the rate at which CN was removed from the aqueous solution (approximately 1 mg CN L^{-1}). At the optimal temperatures of 30°C and 32°C for Chinese elder and weeping willow, respectively, metabolism rates were three-fold (12.6 mg CN kg^{-1} h^{-1}) and five-fold (9.72 mg CN kg^{-1} h^{-1}) higher than at 11°C (Yu et al., 2005).

The evidence suggests that phytoremediation could potentially be feasible for land contaminated with CN from gold-mining activities. In light of the demonstrated potential of plants for CN remediation, and because plants have limited CN tolerance and do not prevent CN uptake through roots in excess of what they can adequately detoxify, the enhancement of plants' natural tolerance to CN would be beneficial in the development of phytoremediation strategies. Genetic engineering could be one way to achieve this enhancement.

1.7 Previous attempts to increase cyanide tolerance in plants

To date, only two studies have attempted to increase the CN detoxification capacity of plants by genetic engineering. Both used the model organism *A. thaliana* and bacterial genes involved in CN metabolism but employed different strategies.

The first attempt was by O'Leary, Preston and Sweetlove (2014) whose focus was to overcome the limits of the *A. thaliana* endogenous CAS detoxification pathway by increasing the capacity for hydrolysis of the toxic β-cyanoalanine intermediate. The logic behind this approach was that if the accumulation of β-cyanoalanine were a limiting factor in the detoxification of CN, an increase in β-cyanoalanine nitrilase activity might then increase the limits of the CN detoxification. They sought to do this through the heterologous expression of *pinA* from *Pseudomonas fluorescens* in *A. thaliana*. pinA, a nitrilase which shares some sequence similarity with plant NIT4, had previously been shown to enable bacteria to use β-cyanoalanine as a sole nitrogen source and grow on toxic concentrations of β-cyanoalanine; be inducible by β-cyanoalanine and, to a slightly lesser extent, its precursors (cysteine and CN); hydrolyse β-cyanoalanine to release ammonia and confer the ability to do the same on other bacteria and Arabidopsis plants deficient in NIT4; and improve β-cyanoalanine tolerance in plants that possessed wild-type NIT4 (Howden, Harrison & Preston, 2009).

Transgenic plants expressing *pinA* grew significantly longer primary roots than wild-type plants in the presence of 10–100 μM KCN and also had greater fresh weight and larger shoots when exposed to

50 µM KCN in agar for 5 days (O'Leary, Preston & Sweetlove, 2014). The reverse was true for the knockdown line, *Atnit4*, which had reduced root lengths and fresh weights than wild-type plants under the same conditions. Furthermore, *pinA* plants exposed to 50 µM KCN had significantly more fresh weight than *pinA* plants grown in the absence of KCN. Wild-type and *Atnit4* in the presence of 50 µM KCN had no change and a significant decrease in fresh weight, respectively, relative to the same plant lines grown in the absence of KCN. During an extended ten-day experiment, *pinA* plants exhibited reduced bleaching of leaves along with an increase in lateral root formation and number and length of root hairs. Feeding with $K^{13}CN$ revealed that *pinA* plants accumulated less β-cyanoalanine and more asparagine (and aspartate to a lesser extent) than wild-type and *Atnit4*, which accumulated a 14-fold higher concentration of β-cyanoalanine than *pinA* and 2.5-fold higher than wild-type. The authors proposed that the reasons for the increased CN tolerance displayed by *pinA* plants may have been a combination of a reduction in the toxic effects of β-cyanoalanine with increased flux through the CAS reaction.

The second attempt was by Kebeish et al. (2015) who employed an approach using a microbial enzyme targeted to the chloroplast and simultaneously overexpressing the endogenous Arabidopsis enzyme that deals with the metabolic products of the bacterial degradation pathway. Specifically, the cyanidase (CynD) from *Pseudomonas stutzeri* was expressed in order to convert CN to formate and ammonia, and endogenous formate dehydrogenase (FDH) was overexpressed for the purpose of converting the formate thus generated to CO_2, leaving the plant with gases it could recycle metabolically (Kebeish et al., 2015). The genes for these proteins were introduced into plants separately (*CynD* or *FDH*) and in combination (*CynD* + *FDH*).

In initial tests in which CN was applied by foliar spray, *CynD* and *CynD* + *FDH* transgenic lines had higher levels of chlorophyll or carotenoid pigments or both; lower levels of catalase, peroxidase and superoxide dismutase antioxidant enzyme activity; and improved growth (rosette size, and fresh and dry weight) compared to the wild-type control plants. For all the parameters tested except dry weight, FDH plants were not significantly different from the control plants. These results were taken as indicators of reduced stress in response to CN in *CynD* and, especially, *CynD* + *FDH* plants. When plants were exposed to 250 µM CN in agar, the authors reported a 56% increase in root length of *CynD + FDH* plants. An increase in internal leaf CO_2 in *CynD* + *FDH* plants compared to control plants was taken as a sign of FDH activity in the former (Kebeish et al., 2015). It might have been informative for the study authors to compare the growth of *CynD* plants with *CynD* + *FDH* at 250 µM CN for the purpose of determining whether the activity of FDH made a significant contribution to the

CN tolerance, over and above the effect of CynD activity. Arguably, it is not sufficient to assume that the growth differences displayed when CN was applied by foliar spray would hold when CN was supplied in the growth medium.

Although the transgenic plants discussed above were capable of significantly better growth in the presence of CN than wild-type *A. thaliana*, their root growth was nevertheless inhibited by the presence of CN. Thus the measure of CN conferred on these plants was incomplete. The study by Kebeish et al. (2015) was one attempt at using efficient microbial enzymes to degrade CN in plants. The present study explored an alternative strategy. Bacterial *CynD* from *B. pumilus* and fungal *CHT* from *N. crassa* were expressed in Arabidopsis. Kebeish et al. (2015) targeted the transgene to the chloroplast in order to make the best use of any CO_2 generated as a result of increased FDH activity. In this study, in addition to the cytoplasmic enzymes, mitochondria-targeted fusion proteins consisting of the nitrilase enzymes with an N-terminal targeting peptide from β-ATPase were also engineered and heterologously expressed in Arabidopsis. The purpose of this was two-fold, being to introduce synthetic metabolic pathways which specifically act on CN as a substrate, detoxify CN in a single step, and produce potentially non-toxic products (compared to some other nitrilases) and to increase the metabolic impact of this intervention by targeting it to a major site of CN toxicity. This would allow a comparison between the cytoplasm and mitochondria as expression sites for CHT and CynD in terms of any enhancement of plant CN tolerance.

1.8 Project aims

The primary aim of this project was to evaluate whether transforming *Arabidopsis thaliana* with either of two genes encoding microbial CN detoxification enzymes would confer on the plants the enhanced ability to grow in the presence of CN. The genes to be used in this study encoded the cyanide hydratase, CHT, from *Neurospora crassa* and cyanide dihydratase, CynD, from *Bacillus pumilus*, respectively. Additionally, it would be determined whether targeting of the enzymes to the mitochondria would improve the ability of transgenic *A. thaliana* to grow in the presence of CN compared to when the enzymes are expressed in the cytoplasm.

To achieve these aims, the following objectives would be pursued:

1. Determine whether the products of CN detoxification by CHT and CynD, formamide and formate, are toxic to *A. thaliana* plants *in vivo*.
2. Establish transgenic *A. thaliana* lines that are homozygous for *CynD* and *CHT*, with the encoded enzymes targeted to either the cytoplasm or the mitochondria.
3. Evaluate the CN tolerance of transgenic *A. thaliana* compared to wild-type.

CHAPTER 2: MATERIALS AND METHODS

2.1 Cloning strategy

Summary

Expression clones containing the *CynD* gene from *Bacillus pumilus* and *CHT* gene from *Neurospora crassa*, with and without mitochondrial-targeting *atpase*, driven by the CaMV 35S promoter were constructed using Gateway® cloning (Invitrogen, Carlsbad, USA). Clones of *CynD* and *CHT* were kindly provided by Professor Trevor Sewell. The genes were amplified from these plasmids using high fidelity *Pfu* DNA polymerase (Promega Corporation, Madison, USA) in a polymerase chain reaction, PCR, incorporating restriction enzyme sites to facilitate subcloning into Gateway® entry vectors' multiple cloning site (MCS); see Table 1 for details of the PCR primers used. Each primer pair was designed to amplify the full coding sequence of its target gene, or a portion thereof (internal primers), using the Sigma DNA calculator (www.sigma-genosys.com/calc/DNACalc.asp). Further details of primer design can be found under the relevant sections of the Results chapter (Chapter 3). PCR-amplified and restriction enzyme-digested DNA were purified either by putting the reaction through the Wizard® SV Gel and PCR Clean-Up System (Promega Corporation) or by agarose gel electrophoresis followed by excision and purification of DNA from the gel slice using the Wizard® kit. For subcloning into entry vectors, a 3:1 insert:vector molar ratio was used for ligation reactions, which were then transformed into *Escherichia coli*. Restriction digests or PCR amplification were used to verify that the insert sequences in plasmids extracted by plasmid minipreparation from the recombinant *E. coli* were of the correct size. The inserts were sequenced to confirm that the integrity of the gene sequence was maintained during subcloning. The verified cDNA clones were then transferred from entry vectors to Gateway® destination vectors using the LR Clonase® reaction (Invitrogen) to produce the final expression clones.

2.1.1 Construction of entry clones

CynD, *atp-CynD* and *atp-CHT* genes were subcloned into pENTR™ 4 (Invitrogen) entry vector using restriction enzyme cloning. *CHT* was subcloned into pENTR™/D-TOPO® (Invitrogen) vector using TOPO® cloning (Invitrogen) according to the manufacturer's instructions. See Results section (Chapter 3) for details of vector construction. Unless otherwise stated, a standard PCR was performed using *Taq* DNA polymerase (Fermentas, Ontario, Canada) in 1X thermophilic DNA polymerase PCR buffer (without $MgCl_2$), 0.2 µM of each primer, 0.2 mM dNTPs (Fermentas) and 1.5 mM $MgCl_2$. Less than 0.5 µg of template DNA was used in each reaction.

Table 1: Primers used in this study.

Primer Name	Sequence	T_a (°C)	Target Sequence Modification
	***CynD* and *CHT* entry clones construction**		
CynD F	5'-GCGGATCCATGACAAGTATTTACCCAAAG-3'	51	5'-*Bam*HI
CynD R	5'-GCCTCGAGTTAAACTTTTTCTTCCAGTATACC-3'		3'-*Xho*I
CHT F	5'-CACCATGGTCCTTACCAAGTACAA-3'	51	5'-CACC
CHT R	5'-TCACTTCTTTCCCTCCTTA-3'		
	***atp-CynD* and *atp-CHT* entry clones construction**		
pBINA5	5'-GGGGATCCATGGCTTCTC-3'	53	5'-*Bam*HI
GFP R	5'-GGGCGGCCGCTTTGTATAGTTCATCCATGCCATG-3'		3'-*Not*I
CynDS F	5'-GCACTAGTATGACAAGTATTTACCCAAAGTTTCG-3'	51	5'-*Spe*I
CynDS R	5'-GCGCGGCCGCTTAAACTTTTTCTTCCAGTATACCATG-3'		3'-*Not*I
CHTS F	5'-GCACTAGTATGGTCCTTACCAAGTACAAGG-3'	51	5'-*Spe*I
CHTS R	5'-GCGCGGCCGCTCACTTCTTTCCCTCCTTATC-3'		3'- *Not*I
	Sequencing of constructs		
pENTR4 F	5'-GCCTTTTTGCGTTTCTACAA-3'		
pENTR R	5'-CAGAGATTTTGAGACACGGG-3'		
attB F	5'-GTACAAAAAAGCAGGC-3'		
attB R	5'-GTACAAGAAAGCTGGG-3'		
pat F	5'-CCAGAAACCCACGTCATGCCAGTT-3'		
pat R	5'-CTACATCGAGACAAGCACGGTCAACTT-3'		
CynD int F	5'-GGAACCGATCAGTGATATGG-3'		
CynD int R	5'-GCTGCTCGAAACTTTGG-3'		
CHT int F	5'-GGTCAGCTCAACTGCTG-3'		
ATP int R	5'-GTTGATGGCTGAGATGC-3'		
	Semi-quantitative and quantitative PCR		
IMPL2 F	5'-GCCATATGGCTTCAAACTCAAAAC-3'	60	
IMPL2 R	5'-GCTCTAGATCAATGCCACTCAAGTGAC-3'		
qCHT F	5'-TCATTAACGAAGCGGGTCAG-3'	59	
qCHT R	5'-CGCGGTACTTCTTCAGCATAG-3'		
qCynD F	5'-AAGATGGCGGTTCTCTCTATTT-3'	57	
qCynD R	5'-CCGGCATCATACTTCCACTT-3'		
qACT2 F	5'-AGT GGT CGT ACA ACC GGT ATT GT-3'	60	
qACT2 R	5'-CAT GAG GTA ATC AGT AAG GTC ACG T-3'		

T_a = annealing temperature

Transformation of *E. coli*

50 µL *E. coli* competent cells, thawed on ice, were added to 1 µL of purified plasmid DNA, mixed and left on ice for 20–30 minutes. The cells were heat-shocked at 42°C for 2 minutes and then placed on ice for 5 minutes. 950 µL Luria-Bertani (LB) broth (1% [w/v] tryptone, 0.5% [w/v] yeast extract, 0.5% [w/v] NaCl) were added to cells and they were incubated with shaking at 37°C for one hour. Transformed *E. coli* were cultured at 37°C overnight on LB agar (1% [w/v] tryptone, 0.5% [w/v] yeast extract, 0.5% [w/v] NaCl, 1.5% [w/v] bacteriological agar) containing selective antibiotics. Kanamycin (50 µg mL^{-1}) was used to select for pENTR4 and pENTR clones, and spectinomycin (100 µg µg mL^{-1}) was used to select for pFAST-G02 clones. A single colony was inoculated into LB broth with antibiotic selection and incubated at 37°C overnight. The recombinant plasmid DNA was extracted from *E. coli* cells in liquid cultures by minipreparation using the Biospin Plasmid DNA Extraction Kit (BioFlux, Bioer, China) and then digested with restriction enzymes to verify the presence of the correct insert. The *pENTR:CHT*, *pENTR4:CynD*, *pENTR4:atp-CynD* and *pENTR4:atp-CHT* entry vectors were double-digested with the restriction enzymes pairs *Bam*HI/*Sac*I; *Bam*HI/*Xho*I; *Spe*I/*Not*I; and *Bam*HI/*Not*I, respectively, to confirm that DNA inserts were the predicted size. The entry constructs were then sequenced.

Agarose gel electrophoresis

Throughout the experiment, DNA was electrophoresed on an agarose gel (1–2% [w/v]) containing 0.016 µg mL^{-1}ethidium bromide in 1X TAE (40mM Tris, 1mM EDTA, 0.11% [v/v] glacial acetic acid) running buffer alongside a DNA ladder (O' Gene Ruler ™ DNA ladder, Fermentas, Ontario, Canada). The gels were then visualized under ultraviolet light (UV). Long wavelength UV (365 nm) was used to prevent damage to the DNA when DNA bands were to be excised from the gel.

DNA sequence analysis

DNA was sequenced using an ABI3730xl DNA analyser (Applied Biosystems, Foster City, USA) at the Stellenbosch University Central Analytical Facility (Stellenbosch, South Africa) or at Macrogen (Seoul, South Korea). DNAMAN (Version 4.13, Lynnon BioSoft, Quebec, Canada) and Chromas (Version 2.01, Technelysium Pty Ltd, Queensland, Australia) software, and the National Center for Biotechnology Information BLAST website were used for analysis of DNA sequencing data. ExPASy (Gasteiger et al., 2003) was used for translating the DNA sequences to protein sequences.

2.1.2 Preparation of expression clones

Preparation of destination vectors

OneShot® (Invitrogen) chemically competent cells were transformed with pFAST-G02 (Shimada, Shimada & Hara-Nishimura, 2010) and cultured overnight on LB agar containing streptomycin (50 µg mL^{-1}) and chloramphenicol (35 µg mL^{-1}). Single colonies were inoculated into LB broth with the same antibiotics. Plasmid DNA extracted from overnight liquid cultures was digested with *Bam*HI to confirm the identity of the vector. The verified pFAST-G02 plasmids were used in LR Clonase® reactions.

LR Clonase® reactions

Four *att*B-containing expression clones, *pFAST-G2:CynD*, *pFAST-G2:atp-CynD*, *pFAST-G2:CHT* and *pFAST-G2:atp-CHT* were formed through *att*L x *att*R recombination reactions between each of the *att*L-containing *pENTR4:CynD*, *pENTR:CHT*, *pENTR4:atp-CHT* and *pENTR4:atp-CynD* entry clones and the *att*R-containing pFAST-G02 destination vector. Each reaction was performed according to instructions in the Gateway® Technology with Clonase™ II manual (Invitrogen). The recombination reaction was incubated at 25°C overnight before the addition of Proteinase K solution. Once complete, 1 µL of the reaction was used to transform *E. coli* (XL1 blue for *CynD* and *CHT*, DH5α for *atp-CynD* and *atp-CHT*). The transformed cells were plated on LB agar containing streptomycin (50 µg mL^{-1}) and incubated overnight at 37°C. Plasmid DNA was extracted from overnight cultures in LB broth containing streptomycin (50 µg mL^{-1}). The presence of the correct insert DNA sequences in the expression vectors was confirmed by amplification of the *CHT*, *CynD*, *atp-CynD* and *atp-CHT* sequences using primer sets CHT F and CHT R; CynD F and CynD R; pBINA5 and CynD R; and pBINA5 and CHT R (Table 1) respectively. The constructs were sequenced and the verified expression clones were used to transform *Agrobacterium tumefaciens* GV3101 (Holsters et al., 1980).

Preparation of *Agrobacterium tumefaciens* GV3101 competent cells

A single colony of *A. tumefaciens* GV3101 was inoculated into 10 mL YEP media (1% [w/v] peptone, 1% [w/v] yeast extract and 0.5% [w/v] NaCl) containing rifampicin (100 µg mL^{-1}) and incubated with shaking overnight at 28°C in the dark. 50 mL fresh YEP media was inoculated with 2 mL of the overnight culture and incubated with shaking at 28°C in the dark until the optical density at 600 nm of the culture measured 0.5–1.0. The culture was chilled on ice before cells were harvested by centrifugation for 5 min at 3000 x *g* at 4°C and suspended in 1 mL ice-cold 20 mM calcium chloride. 100 µL aliquots were dispensed into pre-coooled microcentrifuge tubes, flash-frozen in liquid nitrogen and stored at -80°C.

Transformation of *Agrobacterium tumefaciens* GV3101 with expression vectors

A. tumefaciens GV3101 was transformed with each of purified *pFAST-G2:CynD*, *pFAST-G2:CHT*, *pFAST-G2:atp-CHT* and *pFAST-G2:atp-CynD*. 25 µL plasmid was added directly to frozen competent *A. tumefaciens* GV3101 cells which were then incubated at 37°C for 5 minutes, to thaw and heat shock the cells. 900 µL LB broth were added to the cells and they were incubated shaking at 28°C in the dark for 3–6 h. The cells were then plated onto LB agar containing rifampicin (150 µg mL^{-1}), gentamicin (15 µg mL^{-1}) and spectinomycin (100 µg mL^{-1}) and incubated at 28°C in the dark for two to three days until colonies appeared. Positive transformants were identified by screening single colonies for the presence of the transgenes using colony PCR.

Colony PCR

Colony PCR using Supertherm *Taq* DNA polymerase and previously described primer sets (section 2.1.2) was used to test at least 10 colonies of transformed *A. tumefaciens* GV3101 per construct for the presence of the expression vector. The master mix was prepared and aliquoted according to the Supertherm *Taq* protocol. Each single colony was streaked onto LB agar containing rifampicin (150 µg mL^{-1}), gentamicin (15 µg mL^{-1}) and spectinomycin (100 µg mL^{-1}), and then added to the appropriate PCR tube containing master mix. The PCR products were electrophoresed on 1% (w/v) agarose gels and visualised under ultraviolet (UV) light. The positive transformant colonies' streak plates were incubated for two days at 28°C in the dark. Single colonies were used to grow overnight cultures which were then used to make glycerol stocks of the recombinant *Agrobacterium*.

2.1.3 Glycerol stocks

Glycerol stocks of clones were prepared by mixing 320 µL sterile 50% glycerol and 680 µL overnight liquid bacterial culture, flash-freezing the mixture in liquid nitrogen and storing it at -80°C.

2.2 Generation of transgenic plants

Wild-type *Arabidopsis thaliana* ecotype Columbia-0 (Col-0) plants were transformed by floral dipping as described by Clough & Bent (1998):

Growth of plants on soil

Seeds were sown onto a 1:1 mixture of hydrated peat pellets (Jiffy Products International AS, Norway) and vermiculite, covered in cling-wrap to maintain high humidity, and incubated at 22°C exposed to a 16/8 h light/dark cycle under fluorescent lights (80–100 µmol photon sec^{-1} m^{-2}). Seven days after planting, the cling-wrap was removed and the plants were exposed to a constant relative

humidity of 55%. In preparation for floral dipping, the primary bolt of each plant was cut near its base to promote the growth of multiple secondary bolts. Approximately seven days after cutting, when flower buds were immature and few siliques had formed, the plants were ready for dipping.

Preparation of recombinant *Agrobacterium*

A single colony of recombinant *Agrobacterium* (section 2.1.2), cultured for two days on LB agar containing rifampicin (150 μg mL^{-1}), gentamicin (15 μg mL^{-1}) and spectinomycin (100 μg mL^{-1}), was inoculated into 5 mL LB broth with the same antibiotics and incubated shaking for two days at 28°C in the dark. The 5 mL culture was inoculated into 500 mL LB broth and incubated shaking overnight at 28°C in the dark. Bacterial cells were then harvested by centrifugation at 3500 x *g* for 15 min at room temperature and the cell pellet resuspended in 250 mL 5% (w/v) sucrose containing 0.05% (v/v) Silwet L-77 (Lehle Seeds, Round Rock, USA) surfactant.

Transformation of *Arabidopsis thaliana* with recombinant *Agrobacterium*

Up to 12 *A. thaliana* plants per construct were transformed with *A. tumefaciens* GV3101 carrying *pFAST-G2:CynD*, *pFAST-G2:CHT*, *pFAST-G2:atp-CHT* or *pFAST-G2:atp-CynD*. Empty vector control plants were transformed with pFAST-G02. The inflorescence of each plant was submerged into the sucrose bacterial suspension for 5 seconds. Plant pots were laid on their sides onto trays lined with paper towel moistened with the sucrose bacterial suspension, covered in clingwrap and left overnight at 22°C. The following day, the clingwrap was removed and the plants were set upright and watered. Plants were allowed to grow for 4–6 weeks until mature.

2.2.1 Propagation of transgenic plant lines using BASTA selection

Seed collection and storage

Seeds were collected from dried mature plants, left to dry at room temperature for three to five days and then stored at 4°C.

BASTA selection of positive transformants

The pFAST-G02 vector carries the *bar* gene which confers resistance to BASTA or glufosinate ammonium. Five- to seven-day-old seedlings grown from T_0 seeds were sprayed with 0.015% (w/v) glufosinate ammonium (Duchefa Biochemie, Haarlem, the Netherlands) as described by Weigel and Glazebrook (2002). After the third treatment, plants were allowed two further days of growth before the positive transformants, easily distinguishable from the moribund non-transformants, were

transplanted into a fresh peat and vermiculite mixture, covered in cling-wrap for one night, and grown as normal.

Identification of homozygous plant lines

To identify homozygous plant lines, 100 T_2 seeds were sown in a single pot per plant line and sprayed with BASTA as previously described. The ratio of survivors to non-survivor plants for each plant line was determined. Homozygous plant lines were determined to be those with ≥96% survivors. For these plant lines, another round of screening with BASTA using 20 T_2 seeds per pot was used to confirm that the ratio of survivors remained the same.

2.2.2 Genotyping of transgenic plants

DNA extraction

DNA was extracted from *A. thaliana* leaf tissue using the protocol described by Edwards, Johnstone & Thompson (1991).

PCR detection of *CHT* and *CynD* in transgenic plant DNA

CHT F and CHT R; pBINA5 and CHT R; CynD F and CynD R; and pBINA5 and CynD R primer pairs were used to amplify *CHT*, *atp-CHT*, *CynD* and a*tp-CynD* genes, respectively, from extracted transgenic plant DNA, to confirm that the transgenes had been incorporated into the genome. DNA from wild-type *A. thaliana* Col-0 and from plants transformed with the empty vector, pFAST-G02, served as controls. Primers pat F and pat R were used to amplify the pFAST-G02 MCS region from empty vector control plant DNA.

2.2.3 Transgene expression analysis

RNA extraction and electrophoresis

RNA was extracted from frozen leaf tissue by homogenising in TRIzol extraction buffer (0.1 M sodium acetate pH 5.2, 0.8 M guanidine thiocyanate, 0.4 M ammonium thiocyanate, 5% [v/v] glycerol, 38% [v/v] phenol pH 4) according to the TRIzol® Reagent protocol (Invitrogen). The extracted RNA was resuspended in DEPC-treated water. The RNA was treated with DNase (Turbo DNA-*free*™ Kit TURBO™ DNase Treatment and Removal Reagents, Ambion, Carlsbad, USA) according to the manufacturer's instructions. For each reaction, 2.5 µg RNA were incubated with 2 units (1 µL) of TURBO DNase in a total volume of 20 µL. RNA samples (2.5 µg each) were incubated with 0.2 volumes of sample application buffer (4X MOPS [0.4 M MOPS, 0.1 M sodium acetate, 10 mM EDTA pH7], 2.7% [v/v] formaldehyde, 30.8% [v/v] formamide, 20% [v/v] glycerol and 0.01 mg mL^{-1} EtBr) at

65°C for 5 min, snap-cooled on ice and then electrophoresed in a formaldehyde denaturing gel (1.2% w/v agarose, 1X MOPS, 2.25% v/v formaldehyde) in 1X MOPS running buffer. The RNA bands were visualised under UV to verify that the RNA had not degraded during extraction. RNA was quantified and the $A_{260/280}$ and $A_{260/230}$ ratios determined using a Nanodrop ND-100 Spectrophotometer (Nanodrop Technologies, Wilmington, USA).

cDNA synthesis by reverse transcription-PCR

1–2 µg of DNase-treated RNA was used as a template in a PCR using Superscript™ III Reverse Transcriptase (Invitrogen) according to the manufacturer's protocol with the following alterations: sterile water was substituted for RNaseOUT™ and for half of the enzyme volume. The cDNA produced was tested for integrity and genomic DNA contamination by Supertherm *Taq* PCR amplification of the *IMPL2* gene (*MYO-INOSITOL MONOPHOSPHATASE LIKE 2; At4g39120)* with IMPL2 F and IMPL2 R primers (Table 1). The PCR product size for *IMPL2* from genomic DNA, gDNA, is larger than that from complementary DNA, cDNA, thus allows the detection of any contaminating gDNA. The presence of the transgene sequence in the cDNA was determined by Supertherm *Taq* PCR amplification with the primer sets CynD F and CynD R; CHT F and CHT R; pBINA5 and CynD R; and pBINA5 and CHT R (Table 1). Genomic Col-0 DNA was also tested with these transgene-specific primers. For each transgene, a pool of cDNA from the different plant lines was diluted ten-fold if 2 µg RNA were used, or five-fold if 1 µg RNA was used as a template for RT-PCR reactions. The pooled cDNA was used for semi-quantitative and real-time quantitative PCR.

Semi-quantitative PCR

Magnesium titration and amplification cycle number optimisation PCRs were performed to determine the linear range of PCR product formation from each cDNA pool template. CynD F and CynD R primers were used to amplify *CynD* and *atp-CynD* templates. CHT F and CHT R primers were used to amplify *CHT* and *atp-CHT* templates. Once optimal conditions had been identified using the cDNA pool, cDNA from each of the separate plant lines was used as template in PCR. The PCR products were electrophoresed in 1% (w/v) agarose gels and the DNA bands visualised under UV light. In this way, plant lines displaying high and low levels of transgene expression relative to each other were identified.

Real-time quantitative PCR

Serial dilutions of the pooled cDNA were used to construct a standard curve to determine the linear range for quantitative PCR (qPCR) amplification using primers specific to the gene of interest and

reference gene primers. Primers for quantitative PCR were designed using the PrimerQuest tool from the Integrated DNA Technologies website (https://eu.idtdna.com/Primerquest/Home/Index). qCynD F and qCynD R primers (Table 1) were used for *CynD* and *atp-CynD* templates with an annealing temperature of 57°C. qCHT F and qCHT R primers (Table 1) were used for *CHT* and *atp-CHT* templates with an annealing temperature of 59°C. The forward and reverse primer in each of these pairs was used at a final concentration of 200 nM. qACT2 F (Schenk et al., 2003) and qACT2 R primers were used to amplify the *ACTIN2* reference gene with an annealing temperature of 60°C. The final primer concentrations used were 900nM and 300nM for the forward and reverse primers respectively. The qPCRs were performed using the KAPA SYBR® Fast Master Mix (KAPA Biosystems, Boston, USA) according to the manufacturer's instructions, in a total volume of 10 µL. The following cycling conditions were used: 95°C for 3 min followed by 40 cycles of 95°C for 3 s, annealing temperature for 20 s, 72°C for 1 s. This was immediately followed by the generation of melting curves. cDNA samples from individual plant lines were then diluted to a concentration falling within the established linear range of the standard curve, from which the transgene expression was determined using the same qPCR parameters. In this way, the relative expression of the transgene in different plant lines was determined.

2.3 Assessment of transgenic plant growth in the presence of cyanide

2.3.1 Growth of wild-type *A. thaliana* in the presence of formate and formamide

Growth of plants on MS agar

Agar (0.7% [w/v] bacteriological agar) containing half-strength Murashige and Skoog medium with vitamins (Highveld Biological, Lyndhurst, South Africa), hereafter referred to as MS agar, at pH 5.7 was used to grow *A. thaliana* plants. Seeds were sterilized by washing in 70% (v/v) ethanol with shaking for 5 min, followed by four 5 min washes in sterile Milli-Q water. The seeds were then resuspended in 0.1% (w/v) agar or water. The agar/water seed suspension was pipetted onto the surface of the MS agar. The agar plates were stratified at 4°C in the dark for two days before incubation for seven days at 22°C and 55% relative humidity under a 16/8 h light/dark cycle. The plates were incubated horizontally.

Preparation of formate and formamide MS agar plates

7.5 M sodium formate was produced by reacting equal volumes of 15 M formic acid with 15 M sodium hydroxide. The reaction was considered to be complete when the reaction pH stabilized at pH 7. MS agar containing 100 mM MES, to buffer the pH at 5.7, was prepared. The appropriate amount of formate and formamide was added to the autoclaved agar just before pouring. Seven-

day-old plants were transferred onto plates containing 0, 0.1, 1, 10 and 100 mM concentrations of either formate or formamide. Plates were incubated horizontally for seven days at 22°C and 55% relative humidity under a 16/8 h light/dark cycle.

Biomass assay

Plants grown on MS agar containing formate and formamide for seven days were cut at the base of the shoot, just above the agar surface, and blotted to remove any excess water or agar. The fresh weight of individual shoots was measured. Three shoots per concentration of formate or formamide were used.

Growth of plants in hydroponics media

A. thaliana Col-0 seeds were germinated on rock wool in microfuge tubes as described by Gibeaut et al. (1997) except that water was used for germination instead of Gibeaut's solution. Hydroponics chambers were constructed by painting 4.5 L plastic storage containers with black paint to block out light overlaid with white paint to prevent overheating under the fluorescent lights. The lids of the storage containers were pierced using a heated cork-borer to form a uniform grid of holes into which the microfuge tubes could be slotted without falling through. After seven days, seedlings were transferred from the water to hydroponics chambers containing enough Gibeaut's solution (pH 6.0) to touch the base of the microfuge tubes. 7–10 seedlings were transferred to Gibeaut's solution containing 0, 0.1, 1, 10 and 100 mM formate or formamide and grown at 22°C and 55% relative humidity under a 16/8 h light/dark cycle. Seven plants per concentration of formate or formamide were allowed to grow for 14 days before shoots were removed by cutting at the base, above the rock wool surface, and blotted to remove any excess moisture. The shoots were allowed to dry overnight in a 60°C oven and dry shoot and root biomass was measured.

2.3.2 Cyanide tolerance assays

Root elongation assay

A. thaliana Col-0 seeds were germinated on vertical MS agar (0.8% [w/v] agar, pH 7) plates for seven days at 22°C and 55% relative humidity under a 16/8 h light/dark cycle. Seedlings were transferred to MS agar (0.8% [w/v] agar, pH 7) plates containing 0–100 µM potassium cyanide in order to construct a dose-response curve. A 40X stock solution of potassium cyanide (400 mM KCN in 100 mM NaOH) was diluted in 25 mM NaOH to a 40 mM KCN working solution. The exact volume of potassium cyanide required for the desired concentration in a final volume of 50 mL MS agar was pipetted into the bottom of the petri dish. 50 mL of 42°C MS agar were pipetted into the petri dish.

The agar was mixed with the potassium cyanide solution and allowed to set. Ten seedlings per concentration for each plant line were transferred from the germination plates onto the cyanide-containing plates as quickly as possible to avoid the loss of cyanide as HCN. Once a plate was completed, it was sealed with Parafilm® before proceeding to the next plate. Two plates per concentration were used. When all the plates were complete they were each double-wrapped in electronic insulation tape. The bottom of each plant root was marked before plates were incubated vertically in a growth chamber at 22°C and 55% relative humidity under a 16/8 h light/dark cycle. Seven days later, the plates were removed from the growth chamber, the new position of the root tip was marked and the plates were photographed. Image J 1.46r software (Eliceiri, Rasband & Schneider, 2012) was used to measure the length of roots from the photographs taken. From this experiment, a potassium cyanide concentration was selected for screening of transgenic plant lines. See Results section (Chapter 3) for details.

Germination assay

A. thaliana Col-0 and transgenic seeds were sterilised by washing in 70% ethanol for five minutes then rinsing in absolute ethanol. The absolute ethanol seed suspension was tipped onto filter paper and allowed to dry in the laminar flow cabinet. Seeds were then sprinkled onto plates (four plant lines per plate) taking care to ensure that cross-contamination between plant lines did not occur. Plates were sealed with Parafilm® and electrical insulation tape at the end of the experiment as previously described. The plates were stratified at 4°C in the dark for two days then transferred to growth chambers at 22°C and 55% relative humidity under a 16/8 h light/dark cycle. Germination was scored at 2, 8 and 14 days after transfer to 22°C using an Olympus (SZ2-ILST) dissecting microscope (Olympus Corporation, Tokyo, Japan). At day 2, germination was marked by radicle emergence from the seed coat. At day 8 and day 14, germination was marked by formation of unfolded true leaves and root length greater than 1 cm. The experiment was repeated using transgenic plant lines.

2.4 Data analysis

Statistical analysis of the data from this work was performed using Microsoft Excel 2013 Data Analysis Toolpak.

CHAPTER 3: RESULTS AND DISCUSSION

3.1 Introduction

Bacillus pumilus and *Neurospora crassa* have very efficient CN detoxification mechanisms. For example, *B. pumilus* has been shown to degrade concentrations of free cyanide (supplied as KCN) as high as 100 mg CN L^- (4 mM CN) (Meyers et al., 1991). CynD converts CN to formate and ammonia in *B. pumilus* and CHT converts CN to formamide in *N. crassa* (Ebbs, 2004).

Vectors were constructed containing either *CynD* or *CHT* for heterologous expression of these enzymes in *A. thaliana*. A major toxic effect of CN stems from its action on the electron transport chain in the mitochondria therefore expression constructs encoding the same enzymes with a mitochondrial targeting peptide were also made. *CynD* and *CHT* were separately introduced into *A. thaliana* to test whether they could augment the endogenous CN detoxification system to increase CN tolerance in this species.

3.2 Construct assembly

3.2.1 Construction of *pENTR4*:*CynD* and *pENTR*:*CHT* entry clones

Amplification of *CHT* and *CynD* from cDNA clones

E. coli DH5α harbouring cDNA clones of *CynD* and *CHT* were provided on agar plates by Professor Trevor Sewell. Single colonies from each plate were inoculated into LB containing kanamycin (50 µg mL^{-1}) and incubated overnight at 37°C with shaking. Plasmid DNA was extracted, double-digested with appropriate restriction enzymes and then electrophoresed in a 1.2% agarose gel to verify the plasmids. The *CHT* plasmid was digested using *Eco*RI and *Xba*I. The *CynD* plasmid was digested with *Xho*I and *Xba*I.

PCR primers were designed to add 5'-*Bam*HI and 3'-*Xho*I restriction sites to the 993 bp *CynD* coding sequence DNA, and 5'-CACC (without 3' modification) to the 1056 bp *CHT* coding sequence DNA. These were CynD F and CynD R; and CHT F and CHT R, respectively (Table 1). *CynD* and *CHT* DNA was PCR-amplified from the verified plasmids using high fidelity *Pfu* DNA Polymerase (Promega Corporation), according to the manufacturer's instructions, with an annealing temperature of 51°C. The PCR products were electrophoresed in a 1.2% agarose gel to verify the amplicon sizes.

Construction of *pENTR4*:*CynD*

One microgram of purified *CynD* amplicon was double-digested with *Bam*HI/*Xho*I and purified. Three micrograms of pENTR™ 4 vector were digested with the same restriction enzymes and then electrophoresed in a 1.2% (w/v) agarose gel. The linearized pENTR4 backbone DNA (lacking the *ccd*B gene) was gel-purified and ligated to *Bam*HI/*Xho*I-digested *CynD* (65 ng) (Figure 4A).

E. coli XL1 blue were transformed with the ligation reaction, plated on LB agar containing kanamycin (50 µg mL^{-1}) and incubated overnight at 37°C. Single colonies were then inoculated into LB containing kanamycin (50 µg mL^{-1}) and incubated overnight at 37°C with shaking. *pENTR4:CynD* DNA was extracted from the overnight cultures and digested with *Bam*HI/*Xho*I to release the *CynD* insert as confirmation of a successful ligation (Figure 5). The *CynD* insert in *pENTR4:CynD* clones was sequenced using pENTR4 F and pENTR R primers (Table 1) to confirm that no mutations had been introduced during the PCR amplification.

Construction of *pENTR*:*CHT*

The *CHT* sequence contains the same restriction sites as the pENTR™ 4 multiple cloning site, therefore, TOPO® Cloning was used as an alternative to restriction enzyme cloning. 1.5 ng of purified *CHT* amplicon DNA was directionally inserted into pENTR™/D-TOPO® Gateway® entry vector by TOPO® Cloning (Figure 4B). *E. coli* XL1 blue were transformed with the entire reaction mixture, plated on LB containing kanamycin (50 µg mL^{-1}) and incubated overnight at 37°C. *pENTR:CHT* plasmid DNA was extracted from overnight cultures and digested with *Bam*HI/*Sac*I as a diagnostic digest (Figure 6). *pENTR:CHT* clone insert DNA was sequenced using M13 F and M13 R primers to confirm its identity and the absence of any PCR-introduced mutations.

3.2.2 Construction of *pENTR4*:*atp-CynD and pENTR4*:*atp-CHT* clones

Construction of *pENTR4*:*atp-gfp*

pBIN*mgfp5-atpase* (Logan & Leaver, 2000) was kindly provided by David Logan. *atp-gfp* DNA, which encodes a GFP protein with an N-terminal mitochondrial targeting peptide from *Nicotiana plumbaginifolia* β-ATPase, was PCR-amplified from pBIN*mgfp5-atpase* with primer set pBINA5 (Logan & Leaver, 2000) and GFP R (Table 1) using *Pfu* DNA Polymerase. The primers added 5'-*Bam*HI and 3'-*Not*I restriction sites, respectively. The PCR products were electrophoresed in a 0.8% agarose gel to confirm the presence of *atp-gfp* (Figure 7) and digested with *Bam*HI/*Not*I. Three micrograms of pENTR™ 4 were digested using *Bam*HI/*Not*I and the digest products were separated by electrophoresis in a 1% agarose gel. Purified *Bam*HI/*Not*I-digested *atp-gfp* DNA was ligated into the

gel-purified pENTR4 *Bam*HI/*Not*I backbone to generate *pENTR4:atp-gfp* (Figure 4C). Purified *pENTR4:atp-gfp* plasmid DNA was digested using *Bam*HI/*Not*I and electrophoresed in a 1% agarose gel to verify the construction of this vector (Figure 8).

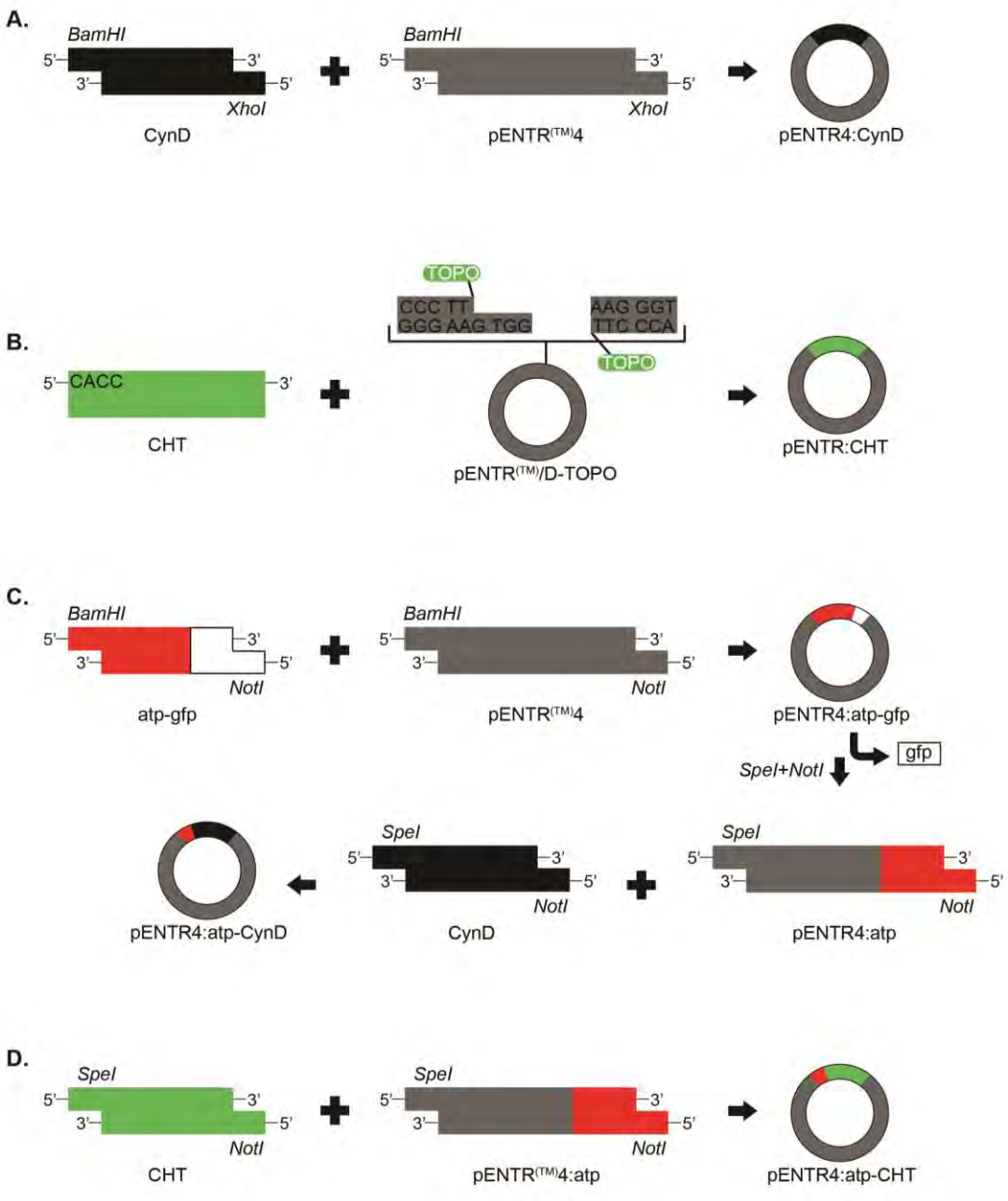

Figure 4: Simplified schematic representation of the construction of entry clones. Restriction enzyme cloning and TOPO cloning were used to construct clones carrying either *CynD* from *B. pumilus* or *CHT* from *N. crassa* without (A and B) and with (C and D) a mitochondrial targeting presequence (*atp*).

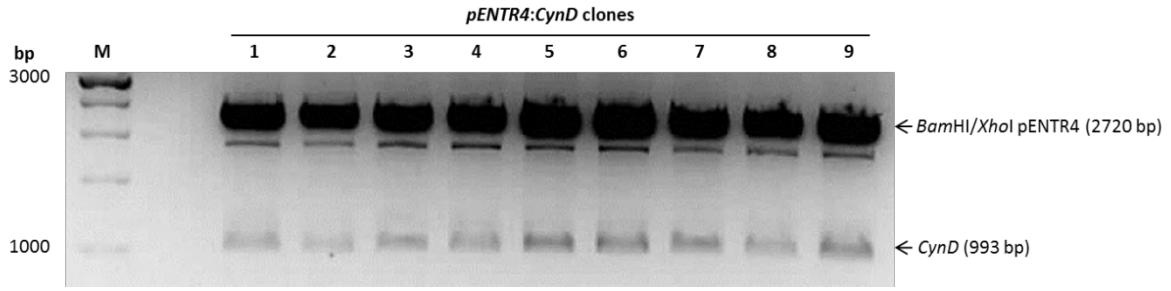

Figure 5: *pENTR4:CynD* clones digested with *Bam*HI/*Xho*I. All clones tested contained a ≈1 kb fragment corresponding to the size of the *CynD* coding region, indicating that *CynD* was successfully ligated into pENTR4. **M**: Molecular size marker DNA; **1–9**: Plasmid DNA purified from nine *E. coli* XL1 blue colonies containing the products of the ligation.

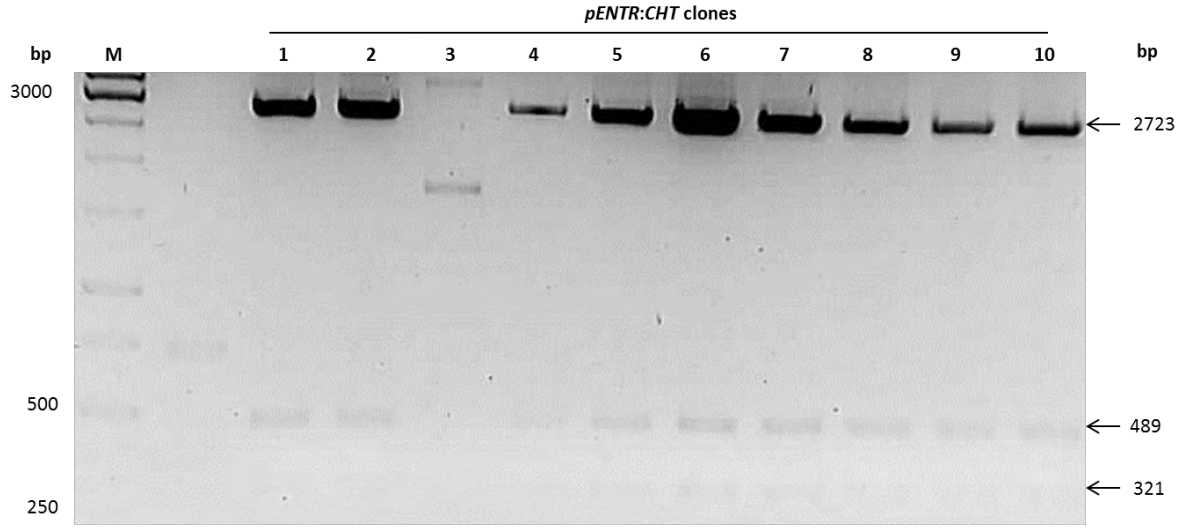

Figure 6: *pENTR:CHT* clones digested with *Bam*HI/*Sac*I. All clones except clone 3 contained fragments with approximate sizes corresponding to the 321 bp, 489 bp and 2723 bp fragments predicted for the cleavage of *pENTR:CHT* by *Bam*HI and *Sac*I, indicating that *CHT* was successfully inserted into pENTR™/D-TOPO® by TOPO® Cloning. **M**: Molecular size marker DNA; **1–10**: Plasmid DNA purified from ten *E. coli* XL1 blue colonies containing the products of the TOPO® Cloning reaction.

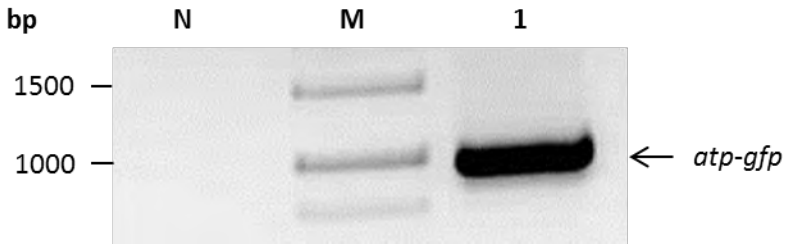

Figure 7: *atp-gfp* DNA, PCR-amplified from pBIN*mgfp5-atpase* (with incorporated 5'-*Bam*HI and 3'-*Not*I restriction sites). A single ≈1 kb PCR product, corresponding to the size of the *atp-gfp* region of pBIN*mgfp5-atpase,* was observed. **N**: No template control; **M**: Molecular size marker DNA; **1**: *atp-gfp* amplicon.

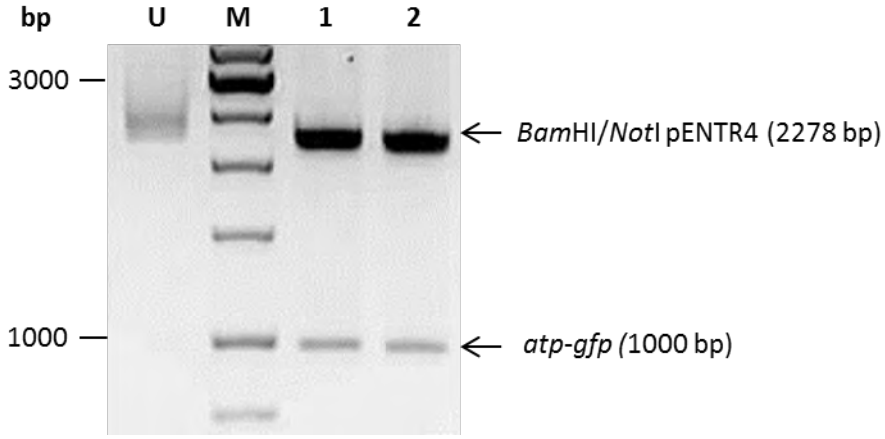

Figure 8: *pENTR4:atp-gfp* digested with *Bam*HI/*Not*I to release the *atp-gfp* insert. The presence of a ≈1 kb band, corresponding to the size of the *atp-gfp* insert, in the digest products confirmed that construction of the vector was successful. **U**: Uncut *pENTR4:atp-gfp*; **M**: Molecular size marker DNA; **1 & 2**: Duplicate digests of *pENTR4:atp-gfp*.

Construction of *pENTR4:atp-CynD*

Three micrograms of *pENTR4:atp-gfp* were digested with *Spe*I/*Not*I to release the *gfp* fragment and the digest products were electrophoresed on a 1% gel (Figure 9). The *pENTR4:atp* backbone DNA was excised from the gel and purified.

CynD and *CHT* DNA was PCR-amplified from the original source plasmids (section 3.2.1) using CynDS F and CynDS R, and CHTS F and CHTS R primers (Table 1), respectively. Both primer pairs introduced 5'-*Spe*I and 3'-*Not*I restriction sites to their respective target gene amplicons.

Two micrograms of purified PCR-amplified *CynD* were digested with *Spe*I/*Not*I and the *CynD* fragment was ligated into *pENTR4:atp* (Figure 4C). *pENTR4:atp-CynD* plasmid DNA was extracted from overnight cultures and digested with *Spe*I/*Not*I to release the *CynD* fragment as verification of

the construction of this vector (Figure 10). *pENTR4:atp-CynD* clone insert DNA was sequenced using pBINA5 and CynD R primers. Internal sequencing primers were used to confirm that the *CynD* coding sequence was in frame with the *atp* mitochondrial targeting sequence.

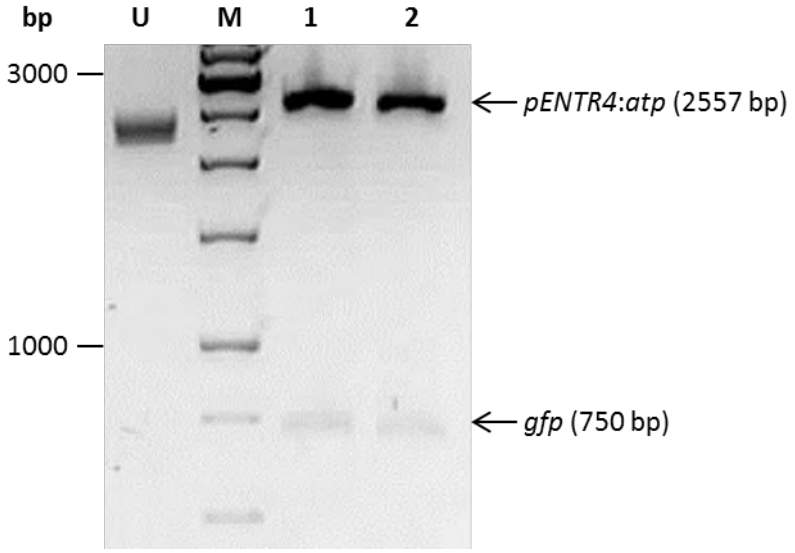

Figure 9: *pENTR4:atp-gfp* digested with *Spe*I/*Not*I to release the *gfp* fragment. The presence of a ≈750 bp band corresponding to the size of the *gfp* fragment confirmed that *gfp* had been released from the vector, leaving a fragment between 2500 and 3000 bp corresponding to the size of the *pENTR4:atp* vector backbone (2557 bp). **U:** Uncut *pENTR4:atp-gfp*; **M**: Molecular size marker DNA; **1 & 2**: Duplicate digests of *pENTR4:atp-gfp*.

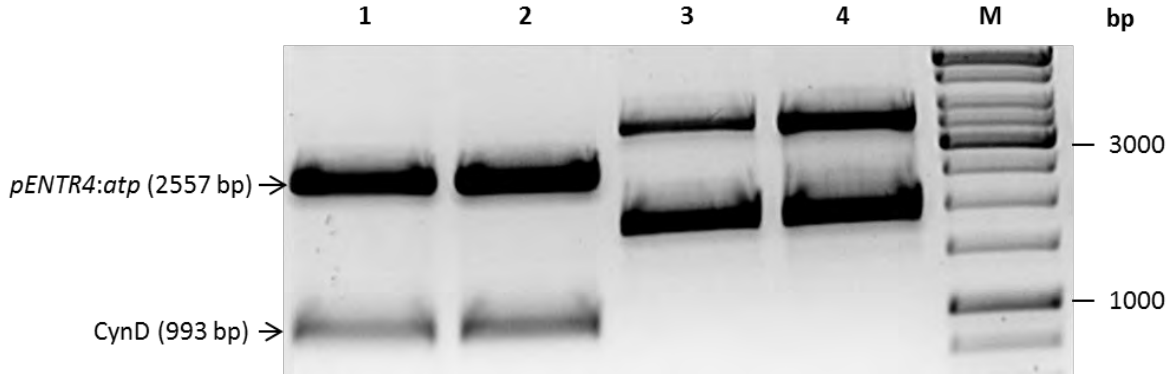

Figure 10: *pENTR4:atp-CynD* clones digested with *Spe*I/*Not*I to release the *CynD* fragment. Clones 1 and 2 contained a ≈1kb fragment corresponding to the size of the *CynD* coding region, confirming that the construction of the vector was successful. **M**: Molecular size marker DNA; **1–4**: Digests of plasmid DNA purified from four *E. coli* colonies containing the products of the ligation of *CynD* to *pENTR4:atp*.

Construction of *pENTR4:atp-CHT*

Purified PCR-amplified *CHT* DNA proved intractable to cloning into *pENTR4:atp* and was therefore subcloned into pGEM®-T Easy (Promega Corporation) to facilitate the process. The DNA was put through an A-tailing procedure as described in the pGEM®-T and pGEM®-T Easy Vector Systems Technical Manual. 250 ng purified *CHT* DNA was adenylated using 0.2 mM dATP in a total reaction volume of 10 µL and the adenylated fragment (50 ng) was then ligated into pGEM®-T Easy vector overnight. Plasmid DNA was extracted, digested with *Eco*RI/*Kpn*I and then electrophoresed on a 1% agarose gel to verify that the ligation was successful. *pGEM-T Easy:CHT* insert DNA was then sequenced with M13 F and M13 R primers.

Three micrograms of *pGEM-T Easy:CHT* were digested with *Spe*I/*Not*I overnight to release the *CHT* insert. The digest products were electrophoresed in a 1% agarose gel and the *CHT* insert was excised from the gel and purified from the gel slice. The purified *CHT* was then ligated into *pENTR4:atp* (Figure 4D) and *pENTR4:atp-CHT* plasmid DNA extracted from overnight cultures was digested with *Bam*HI/*Not*I to confirm the presence of the *atp-CHT* insert (Figure 11). In order to expedite the cloning process, given the additional time taken to construct *pENTR4:atp-CHT*, sequencing of the insert DNA was deferred until the insert was in the final expression clones.

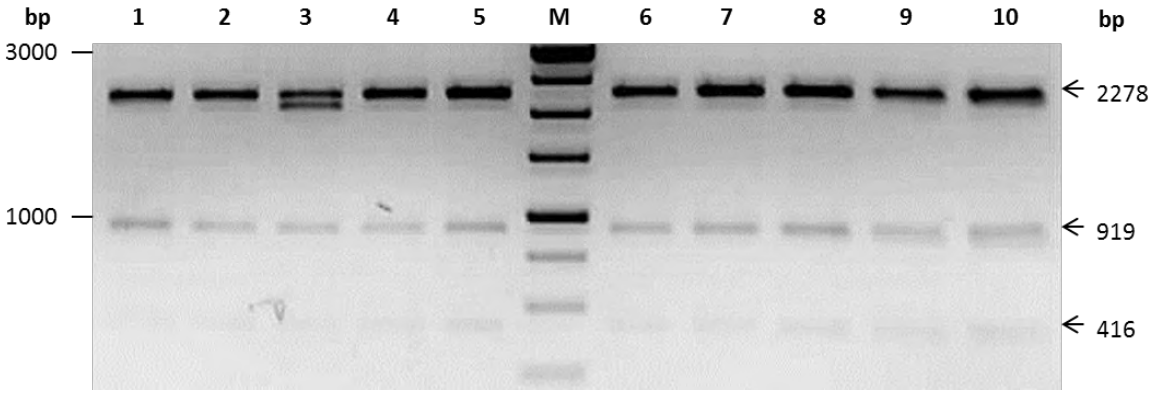

Figure 11: *pENTR4:atp-CHT* clones digested with *Bam*HI/*Not*I. All clones tested contained fragments with approximate sizes corresponding to the 416 bp, 919 bp and 2278 bp fragments predicted for the cleavage of *pENTR4:atp-CHT* by *Bam*HI and *Not*I. *Bam*HI and *Not*I cleaved the sites where the *atp-CHT* fragment was ligated into the vector and *Bam*HI also cleaved once within *CHT*. **M**: Molecular size marker DNA; **1–10**: Plasmid DNA purified from ten *E. coli* colonies containing the products of the ligation of *CHT* to *pENTR4:atp*.

3.2.3 Preparation of expression clones using LR Clonase reactions

In the LR Clonase reaction, 4 *att*B-containing expression clones were formed from *att*L x *att*R recombination reactions between each of the four *att*L-containing entry vectors (*pENTR4:CynD*, *pENTR:CHT*, *pENTR4:atp-CHT* and *pENTR4:atp-CynD*) and the *att*R-containing pFAST-G02 destination vector (Figure 12). pFAST-G02 drives constitutive expression of the gene of interest under the control of the CaMV 35S promoter (Shimada, Shimada & Hara-Nishimura, 2010). Primers CHT F and CHT R; CynD F and CynD R; pBINA5 and CynD R were used to amplify the insert DNA sequences from *pFAST-G2:CHT*, *pFAST-G2:CynD* and *pFAST-G2:atp-CynD* expression clones, respectively, to confirm that the inserts were of the correct size (Figures 13–14). The amplified *atp-CynD* DNA was digested with *Spe*I to separate the *atp* and *CynD* fragments (Figure 15). PCR verification of the *pFAST-G2:atp-CHT* construct was not performed but the insert DNA was sequenced using pBINA5 and CHT R primers. Internal sequencing primers were used to confirm that the coding sequence was in frame with the *atp* mitochondrial targeting sequence in *pFAST-G2:atp-CHT*.

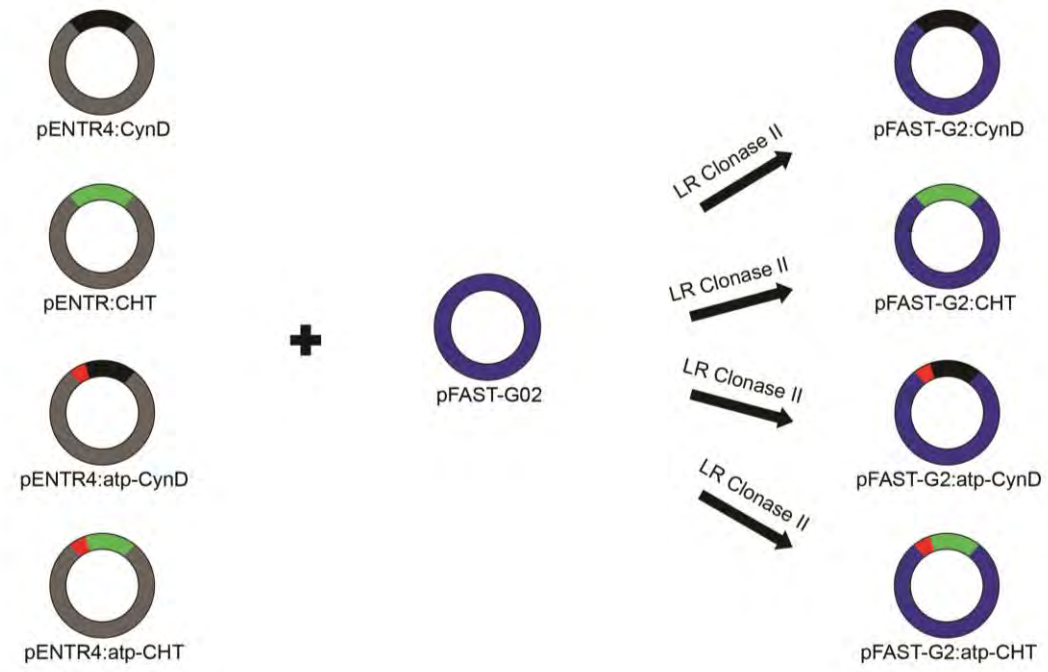

Figure 12: Schematic representation of the construction of expression clones. Insert DNA was transferred from each entry construct to the pFAST-G02 destination vector via a recombination reaction catalysed by LR Clonase II to form the final expression vectors.

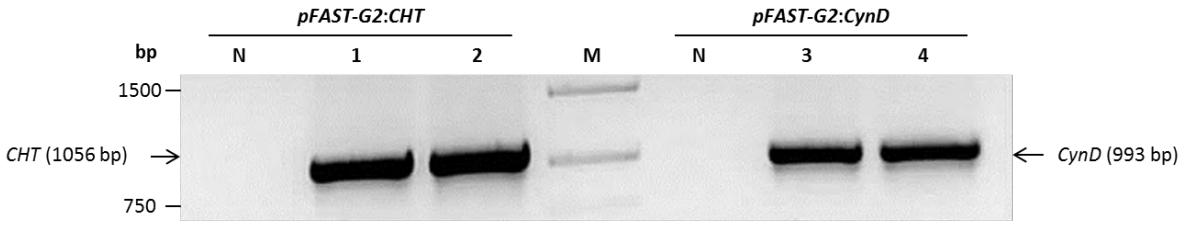

Figure 13: *CHT* and *CynD* DNA, PCR-amplified from *pFAST-G02:CHT* and *pFAST-G02:CynD* expression clones. A single ≈1 kb PCR product in each reaction was observed, corresponding to the sizes of the *CHT* and *CynD* coding regions, indicating the successful formation of the expression vectors. Shown is the amplicon from plasmid DNA purified from two colonies containing the products of the LR Clonase reaction between pFAST-G02 and **1–2**: *pENTR:CHT*; **3–4**: *pENTR4:CynD*. **M**: Molecular size marker DNA; **N**: empty vector control.

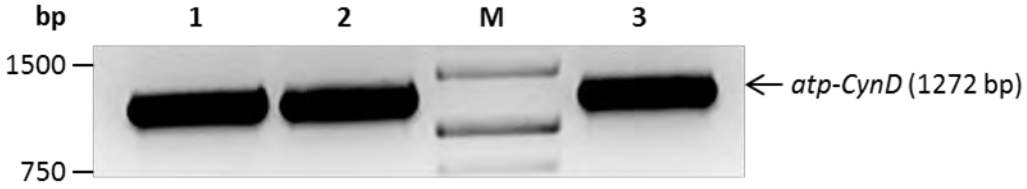

Figure 14: *atp-CynD* DNA, PCR-amplified from *pFAST-G2:atp-CynD* expression clones. A single PCR product corresponding to the size of the *atp-CynD* fragment was observed, confirming the successful construction of the expression vector. **M**: Molecular size marker; **1–3**: Plasmid DNA purified from three *E. coli* colonies containing the products of the LR Clonase-mediated recombination reaction between *pENTR4:atp-CynD* and pFAST-G02.

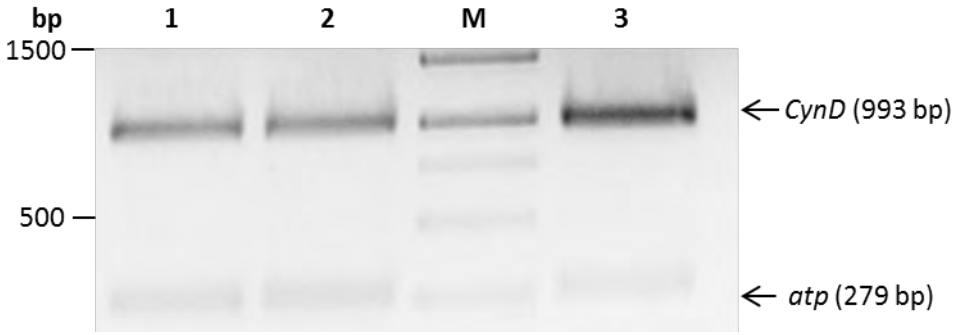

Figure 15: *Spe*I digest of *atp-CynD* amplicon from *pFAST-G2:atp-CynD* expression clones. The presence of bands of ≈1 kb and ≈0.25 kb corresponding to the sizes of the *CynD* coding region and *atp* fragment further confirmed the identification of the amplicon as *atp-CynD*. **M**: Molecular size marker DNA; **1–3**: Digests of amplicons from plasmid DNA extracted from three *E. coli* colonies.

3.3 Verification of recombinant *Agrobacterium* for transformation of *A. thaliana*

Colony PCR was used to confirm the presence of the gene of interest (for each construct) in up to ten recombinant *Agrobacterium tumefaciens* GV3101 clones transformed with the verified expression clones (Figures 16–19). In all cases, the majority of the colonies tested harboured the desired transgene.

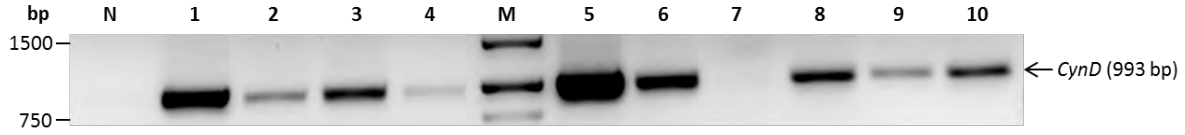

Figure 16: Colony PCR of transformed *A. tumefaciens pFAST-G2:CynD*. Nine out of ten clones tested contained a ≈1 kB fragment corresponding to the size of the *CynD* coding region. **N**: No template control; **M**: Molecular size marker DNA; **1–10**: PCR products from ten colonies.

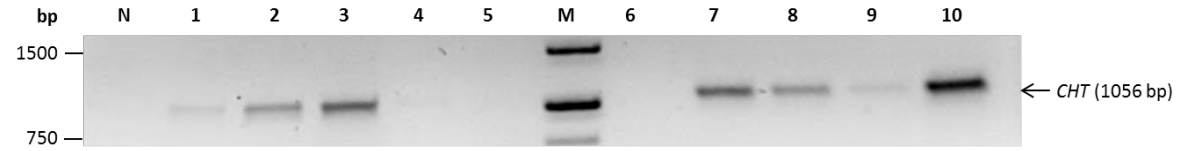

Figure 17: Colony PCR of transformed *A. tumefaciens pFAST-G2:CHT*. Seven out of ten clones tested contained a ≈1 kB fragment corresponding to the size of the *CHT* coding region. **N**: No template control; **M**: Molecular size marker DNA; **1–10**: PCR products from ten colonies.

Figure 18: Colony PCR of transformed *A. tumefaciens pFAST-G2:atp-CynD*. All clones tested contained a fragment, between 1000 and 1500 bp, corresponding to the size of *atp-CynD.* **M**: Molecular size marker DNA; **1–10**: PCR products from ten colonies.

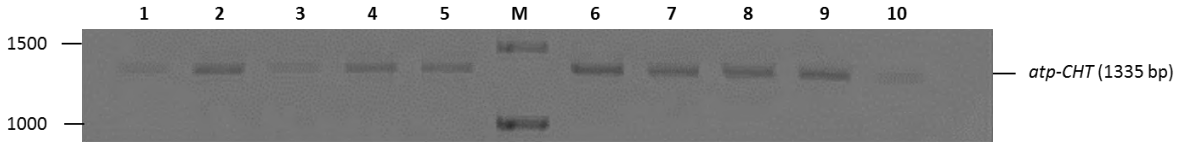

Figure 19: Colony PCR of transformed *A. tumefaciens pFAST-G2:atp-CHT*. All clones tested contained a fragment, between 1000 and 1500 bp, corresponding to the size of the *atp-CHT* fragment. **M**: Molecular size marker DNA; **1–10**: PCR products from ten colonies.

3.4 Characterisation of transgenic *A. thaliana* plant lines

Twelve plants were transformed with each of the expression constructs. Plants were also transformed with the empty pFAST-G02 vector to provide an empty vector control and Col-0 plants served as a wild-type control. *A. thaliana* transformed with *pFAST-G2:CHT*, *pFAST-G2:CynD*, *pFAST-G2:atp-CHT* and *pFAST-G2:atp-CynD* will hereafter be referred to as *CHT*, *CynD*, *atp-CHT* and *atp-CynD* plants. Plants were named as follows: construct, insertion event number (1–12) and plant line number (progeny from a single seed giving rise to a single plant line). For example, *atp-CHT* 10 represents the tenth plant that was transformed with *pFAST-G02:atp-CHT* at T_0. #3 indicates that the particular plant was the third of multiple T_1 progeny.

3.4.1 PCR genotyping of putative transgenic *A. thaliana* T_1 generation

Transgene integration into the genomic DNA was confirmed by PCR amplification from DNA extracted from T_1 plants (Figures 20–23). CHT F and CHT R; CynD F and CynD R; pBINA5 and CHT R; and pBINA5 and CynD R primers were used to amplify the *CHT*, *CynD*, *atp-CHT* and *atp-CynD* transgenes from their respective plant lines. The amplification of a single PCR product confirmed that the transgenes had successfully integrated into the genomic DNA of the parent plants. DNA extracted from Col-0 plants was also amplified with the same sets of primers and it was established that the genes could not be detected in the wild-type DNA (Figures 22 and 23: Col-0 underlined).

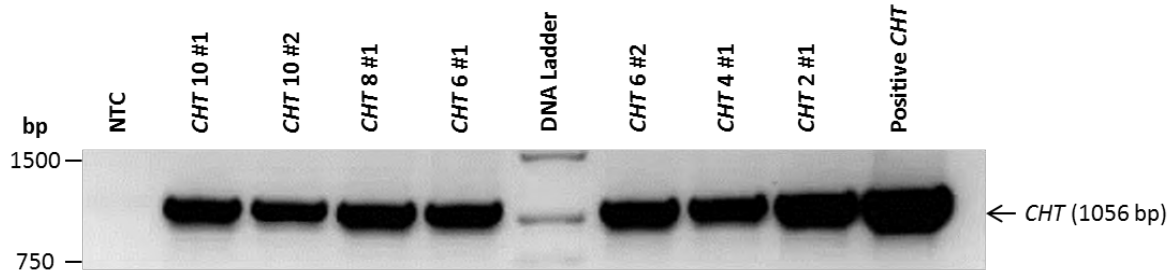

Figure 20: PCR amplification of *CHT* from *A. thaliana pFAST-G2:CHT* T_1 DNA. A single ≈1 kb PCR product corresponding to the size of the *CHT* coding region was amplified from the DNA of each T_1 plant tested, indicating that the transgene was inherited after being successfully incorporated into the genomic DNA of the parent T_0 plants. **NTC**: No template control; **Positive *CHT***: Purified *pFAST-G2*:*CHT* plasmid; ***CHT* 10 #1**: *A. thaliana pFAST-G2:CHT* insertion event line 10, plant line 1 DNA, etc.

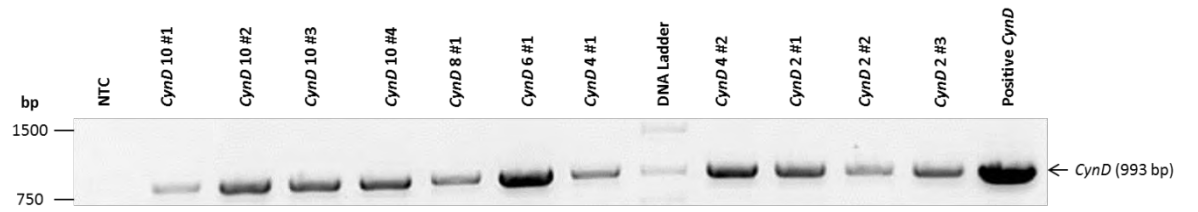

Figure 21: PCR amplification of *CynD* from *A. thaliana pFAST-G2:CynD* T_1 DNA. A single ≈1 kb PCR product corresponding to the size of the *CynD* coding region was amplified from the DNA of each T_1 plant tested, indicating that the transgene was inherited after being successfully incorporated into the genomic DNA of the parent T_0 plants. **NTC**: No template control; **Positive *CynD***: Purified *pFAST-G2:CynD* plasmid. ***CynD* 10 #1**: *A. thaliana pFAST-G2:CynD* insertion event line 10, plant line 1 DNA, etc.

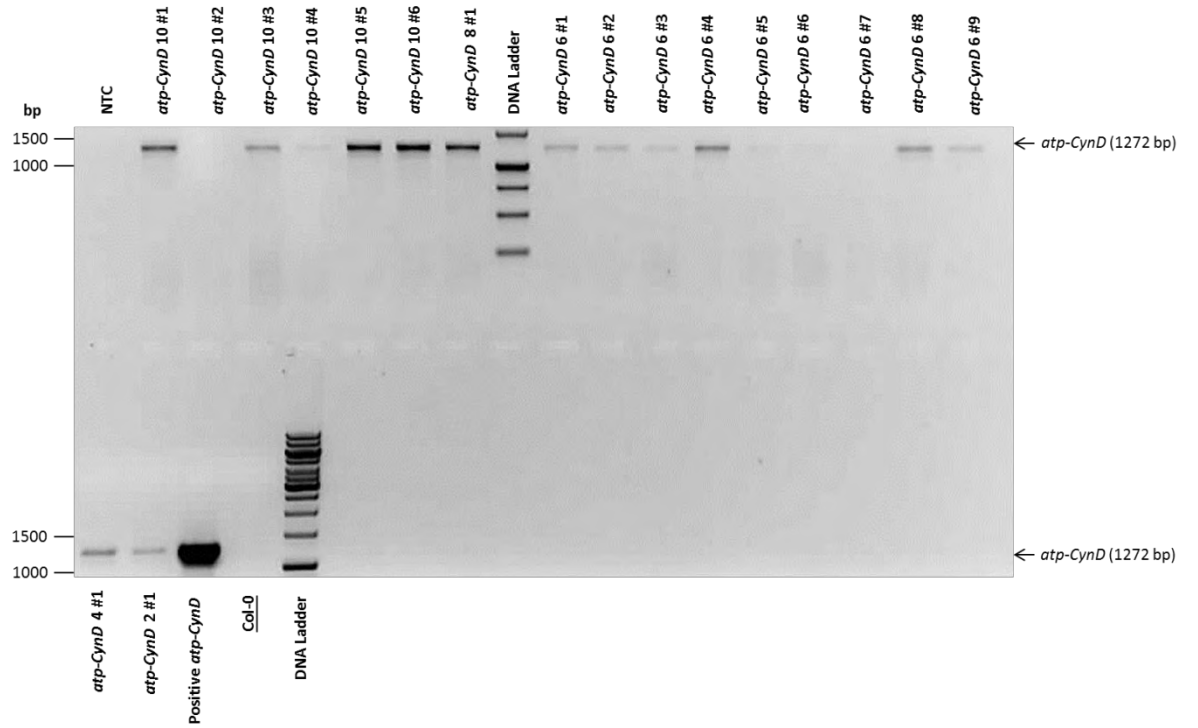

Figure 22: PCR amplification of *atp-CynD* from *A. thaliana pFAST-G2:atp-CynD* T_1 generation. A single product, between 1000 bp and 1500 bp, corresponding to the size of the *atp-CynD* fragment was amplified from the DNA of most of the T_1 plants tested, indicating that the transgene was inherited after being successfully incorporated into the genomic DNA of the parent T_0 plants. *atp-CynD* 10 #2 and *atp-CynD* 6 #7 did not contain the transgene and may have been falsely identified as positive transformants. **NTC**: No template control; **Col-0**: Wild-type *A. thaliana* Col-0 DNA; **Positive *atp-CynD***: Purified *pFAST-G2:atp-CynD* plasmid; ***atp-CynD* 10 #1**: *A. thaliana pFAST-G2:atp-CynD* insertion event line 10, plant line 1 DNA, etc.

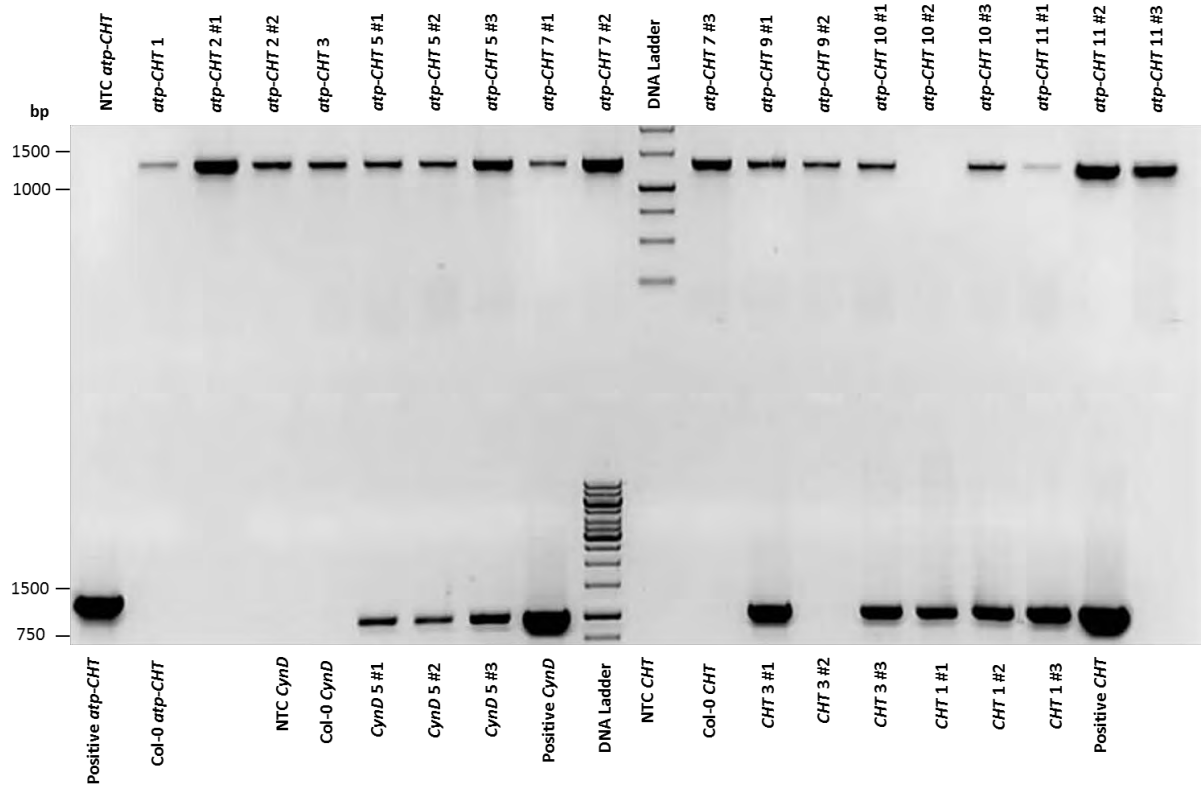

Figure 23: PCR amplification of *atp-CHT*, *CynD* and *CHT* from *A. thaliana pFAST-G2:atp-CHT*, *pFAST-G2:CynD* and *pFAST-G2:CHT* T_1 generations, respectively. A single PCR product was amplified from most of the T_1 plants tested, indicating that the transgenes were inherited after successfully being incorporated into the genomic DNA of the parent T_0 plants. *atp-CHT* 10#2 and *CHT* 3#2 plant lines did not contain the transgenes and may have been falsely identified as positive transformants. **NTC**: No template control; **Positive *atp-CHT*/*CynD*/*CHT***: Purified *pFAST-G2:atp-CHT* plasmid, purified *pFAST-G2:CynD* plasmid and purified *pFAST-G2:atp-CynD* plasmid, respectively; **Col-0 *atp-CHT*/*CynD*/*CHT***: Wild-type *A. thaliana* Col-0 DNA amplified with primers for *atp-CHT*, *CynD* and *CHT* respectively.

3.4.2 Identification of homozygous plant lines using BASTA resistance

Transgenic seeds carrying the pFAST-G2 vector can be identified by the presence of green fluorescence associated with oil body membranes that results from the expression of OLE1-GFP under the control of the *OLE1* promoter (Shimada, Shimada & Hara-Nishimura, 2010). Contrary to expectations, inspection under a fluorescence microscope of seeds harvested from T_2 transgenic plants revealed no detectable GFP fluorescence. Seed fluorescence could therefore not be used as described by Shimada, Shimada & Hara-Nishimura (2010) to determine homozygosity.

Instead, BASTA selection was used to identify homozygous plant lines (section 2.2.1). Of the 181 plant lines tested (up to 10 plant lines per insertion event line for each construct), 38% were found

to be homozygous. Homozygous lines constituted 30%, 53%, 30% and 39% of the *CHT*, *CynD*, *atp-CynD* and *ATP-CHT* plant lines tested, respectively, with the remainder being heterozygous.

3.4.3 Analysis of transgene expression in homozygous *A. thaliana*

The expression of *CHT* and *atp-CHT*; and *CynD* and *atp-CynD* in plants was measured by qPCR amplification of a 129 bp fragment from *CHT* using qCHT F and qCHT R (Table 1) primers and amplification of a 135 bp fragment from *CynD* using qCynD F and qCynD R (Table 1) primers respectively. Each cDNA template used had been synthesized from a pool of total RNA extracted from three separate plants. The two standard curve method was used; the transgene signal was normalized to the *A. thaliana Actin2* (*ACT2*) reference gene signal to obtain the relative expression (Figures 24–25).

atp-CHT expression was detected in all the plant lines tested (Figure 24), confirming that transcription of the transgene had occurred following its integration into the genome. All RNA had been treated with DNase prior to cDNA synthesis to ensure that amplification of the gene of interest from genomic DNA contaminating the cDNA did not occur. *atp-CHT* plant line 10 displayed the highest relative expression of *CHT*, followed by *atp-CHT* 7 and *atp-CHT* 9. *atp-CHT* 3 had the lowest relative expression of *atp-CHT*, which was less than half of that in *atp-CHT* 10.

atp-CynD was also expressed in all the plant lines tested (Figure 25). The highest expressing plant line was *atp-CynD* 3. *atp-CynD* 5 had the lowest expression level, which was less than 10% of that in *atp-CynD* 3. There was only one data point for *atp-CynD* 9, however, given the closeness of the technical replicates for the other plant lines within the same experiment, it was deemed reasonable to assume that the duplicate reaction would have yielded a comparable result.

The target fragment could not be amplified from *CynD* plant cDNA using qCynD primers. This was consistent with the results of semi-quantitative PCR optimization of the qCynD primers which also failed to show amplification from *CynD* cDNA even though there was amplification from *atp-CynD* cDNA (confirming that there were no problems with these primers). Successful amplification of *ACT2* from *CynD* cDNA showed that the failure to amplify *CynD* was not due to RNA degradation occurring prior to cDNA synthesis. Thus, while the transgene was present in the genome, it was apparently not expressed at detectable levels in any of the lines tested. In light of these results, these lines were excluded from further analysis.

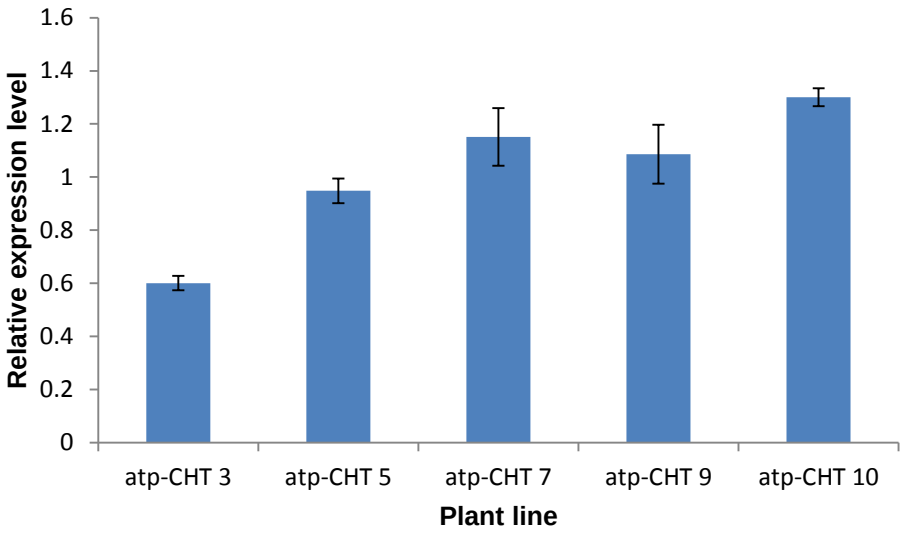

Figure 24: Relative expression of the *CHT* transgene in *A. thaliana atp-CHT* plant lines. The expression level of *CHT* normalized to that of the *Actin2* reference gene for each plant line is shown. Represented is the mean of two technical replicates per sample (pooled cDNA from 3 plants) per plant line. Error bars represent standard deviation.

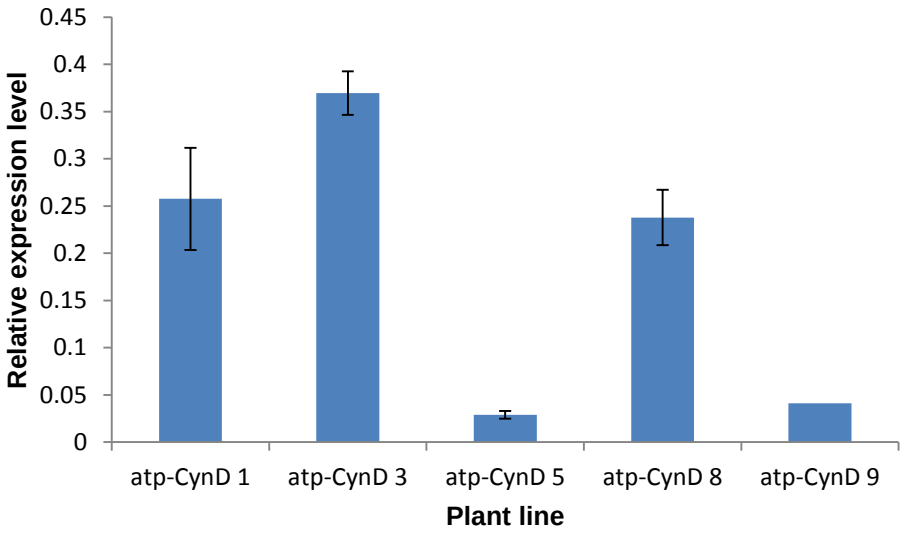

Figure 25: Relative expression of the *CynD* transgene in *A. thaliana atp-CynD* plant lines. The expression of *CynD* normalized to that of the *Actin2* reference gene for each plant line is shown. Represented is the mean of two technical replicates per sample (pooled cDNA from 3 plants) per plant line except for *atp-CynD* 9 (*n* = 1). Error bars represent standard deviation.

The standard curve for quantitation of *CHT* DNA amplified from *CHT* plant cDNA could not be optimised to meet the recommended slope (-3.1 to -3.6) and R-squared (>0.99) values for qPCR (Life Technologies, 2014). Thus, although the standard curve for the quantitation of *ACT2* from the cDNA had been optimised, in the time available, it was not possible to determine the relative expression of *CHT*, only that the transcript was present. These lines were therefore also excluded from further analysis.

3.5 Cyanide tolerance of transgenic *A. thaliana*

3.5.1 Wild-type analysis of response to CynD and CHT metabolic products and cyanide

Effect of formate and formamide on wild-type *A. thaliana* Col-0

As previously discussed, the detoxification of CN by CynD and CHT produces formate and formamide, respectively. Formate is a known to exist in Arabidopsis (Prabhu et al., 1996), for example, as a photorespiratory metabolite formed from the non-enzymatic decarboxylation of glyoxylate (Wingler, Lea & Leegood, 1999). However, it is less clear whether endogenous formamide exists. It was therefore necessary to evaluate the potential toxicity of excess intracellular formate and formamide to transgenic plants expressing functional CynD and CHT. Col-0 seeds were germinated hydroponically in water and after seven days, the seedlings were exposed to formate and formamide at different concentrations in hydroponic growth media to determine whether these metabolites were potentially toxic to the plants.

Exposure to high concentrations (100 mM) of formate and formamide in hydroponic media decreased the biomass of Col-0 plants, suggesting that the formate and formamide were taken up by the roots (Figure 26). After seven days, the shoot and root biomass of plants grown in the presence of 100 mM formate and formamide was approximately 16% and 12%, respectively, of that of the plants grown in normal media and the leaf tissue was bleached. The reduction in biomass in response to formate was observed at a lower concentration than for formamide in shoots but not in roots where the effect was similar. The difference may be a result of formamide being transported less efficiently than formate from roots to shoots.

Interestingly, between 0 and 0.1 mM formate there was an increase in shoot mass but not in roots. Oxidation of the extra formate to carbon dioxide, catalysed by formate dehydrogenase may have been responsible for the increased biomass. The conversion of assimilated exogenous formate to carbon dioxide which is subsequently fed into photosynthesis has been shown to lead to increased fresh weight of rice plants (Shiraishi, Fukusaki & Kobayashi, 2000).

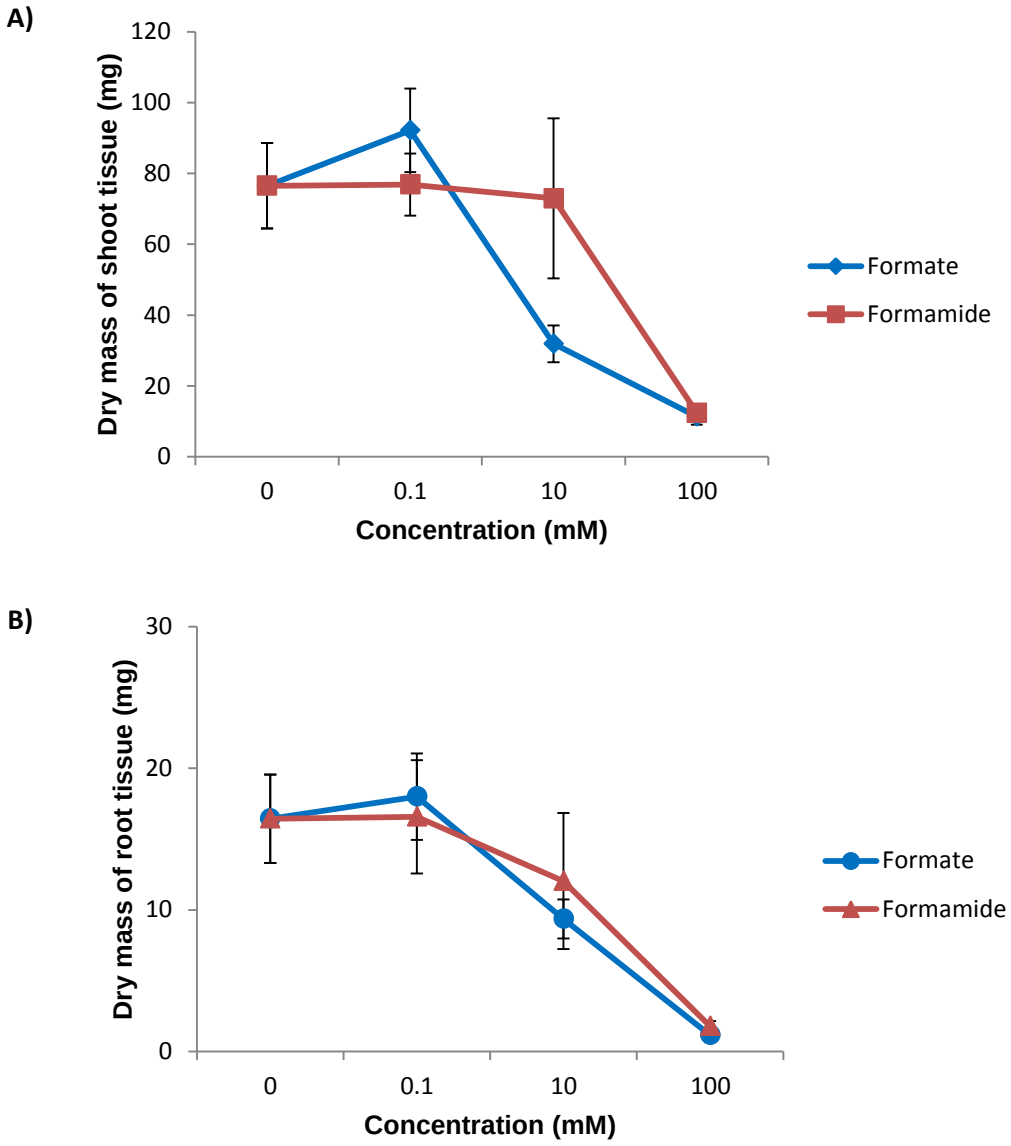

Figure 26: Effect of extracellular formate and formamide on wild-type *A. thaliana* biomass formation. Seven-day-old *A. thaliana* Col-0 seedlings were transferred to formate/formamide-containing media and grown for seven days. Represented is the mean dry mass of the A) shoots and B) roots of plants (*n* = 10) exposed to different concentrations of formate or formamide for seven days. Error bars represent standard deviation.

This experiment showed that, if transgenic plants were to express CynD and CHT enzymes, small increases in intracellular formate and formamide as a result of the enzymes' activity would not necessarily be toxic to the plants and, in the case of CynD, might improve plant growth. Only in excess of 0.1 mM and 10 mM extracellular formate and formamide did the metabolites have a detrimental effect on the plant growth (Figure 26). Although the extracellular concentration is not identical to the intracellular concentration of the metabolites following uptake, this finding is important because toxicity to plants occurs at micromolar concentrations of CN, much lower than the millimolar toxic concentrations of formate or formamide. Therefore transgenic plants expressing these enzymes could potentially benefit from enhanced CN tolerance without any negative formate- or formamide-associated effects on growth.

Effect of KCN on wild-type *A. thaliana* Col-0 plants

The change in tap root length of plants growing on KCN was used to measure the effect of CN on the growth of wild-type *A. thaliana*. Seven-day-old Col-0 seedlings were transferred from normal MS media to MS agar containing 0–200 µM KCN and grown for a further seven days. In excess of 100 µM KCN, root growth on plates was totally inhibited (data not shown) and at 200 µM KCN, the plants were completely bleached. A dose-response curve was therefore constructed using 0–100 µM KCN concentrations (Figure 27). Plates containing the volume of 25mM sodium hydroxide equal to the volume of KCN stock solution used in a 100µM KCN plate were included as the 0 µM KCN control. The growth of the tap root was reduced by 50% between 40 µM and 60 µM KCN, compared to normal media (Figure 27). This was similar to the finding by O'Leary, Preston and Sweetlove (2014) that between 20–50 µM KCN halved root growth compared to normal media.

3.5.2 Analysis of transgenic *A. thaliana* cyanide tolerance

Root elongation on cyanide of transgenic *A. thaliana*

Having established a dose-response curve for wild-type plants, the growth of transgenic *A. thaliana* in the presence of KCN was measured. As a screening test for enhanced growth on KCN compared to Col-0, homozygous transgenic plants were grown on 50 µM KCN. The new tap root growth on 50 µM KCN as a percentage of that on normal MS agar for each transgenic plant line was compared to the wild-type plant growth at the same KCN concentration seven days after transplanting. Transgenic plant lines identified to be potentially more tolerant than the wild-type were selected for dose-response analysis over the range 0–75 µM KCN alongside Col-0.

This method of analysing potential differences in CN tolerance proved to be extremely problematic. While there were indications that some transgenic plant lines were potentially better growers than

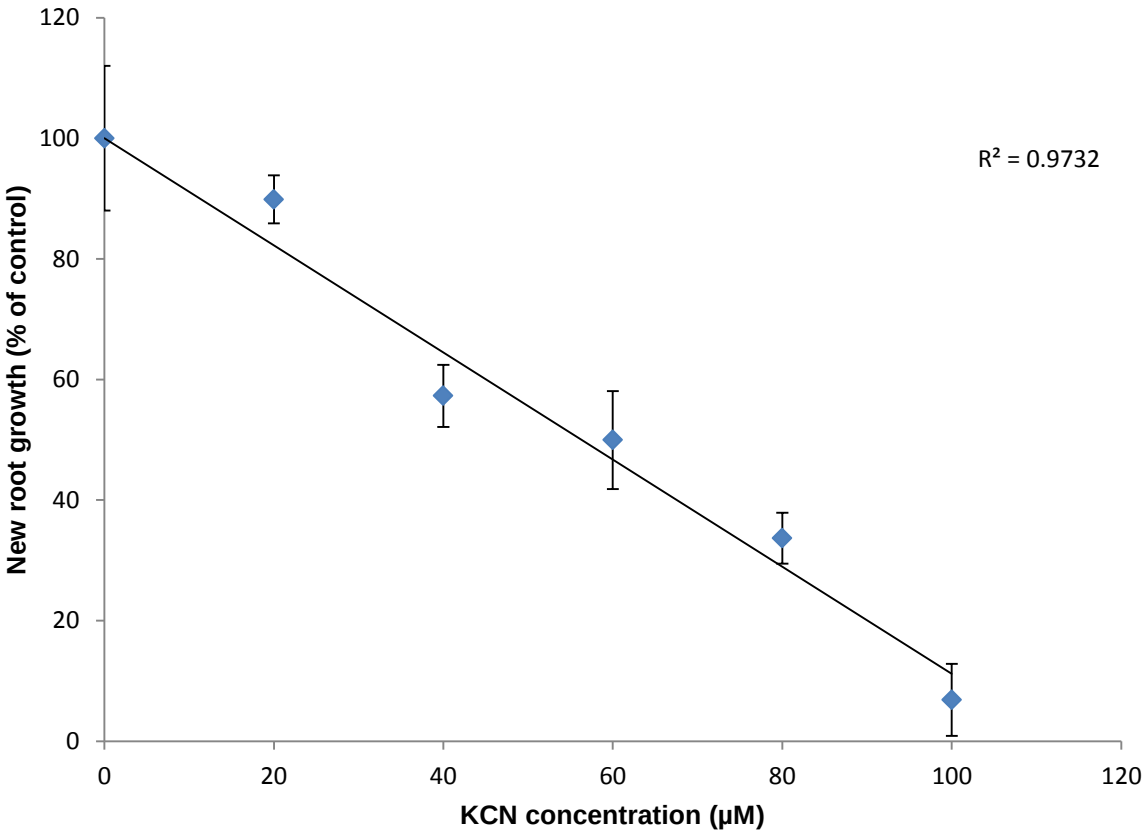

Figure 27: *A. thaliana* root growth dose-response to CN. Seven-day-old *A. thaliana* Col-0 plants were transferred from normal media to agar containing KCN and grown for seven days. Values shown are the mean of the new tap root growth (*n* = 3) after exposure to CN for seven days. Each replicate had 10 plants. Error bars represent standard deviation.

Col-0 when exposed to CN, there was insufficient reproducibility of the results between plates of the same KCN concentration within the same experiment and between the same KCN concentrations in different experiments. Importantly, Col-0 behaved inconsistently as well, making it difficult to draw any conclusions.

Precautionary measures had been taken to maximise the reproducibility of CN tolerance experiments. During the pouring of KCN plates, the temperature of the agar used was kept constant at 42°C to minimise the loss of CN as HCN gas formed due to contact with high-temperature agar. Care was taken to ensure that the KCN solution was uniformly mixed throughout the agar. Even so, transferring plants from the plates they had germinated on to KCN plates may have introduced variation. Specifically, selection bias, damage to roots during transfer, and the amount of time taken to transfer seedlings onto each plate (difference in length of time plates were exposed to air before

being sealed) may have led to differences in plant growth between plates of the same and differing KCN concentrations.

Germination on cyanide of transgenic *A. thaliana*

To develop an alternative assay to test CN tolerance without the need to transfer seedlings, Col-0 seeds were sown directly on KCN-containing media (0–75 µM KCN) to see if they could germinate (measured as radicle emergence). Wild-type seed germination was not inhibited by the presence of KCN, and by day 2, the percentage of seeds displaying radicle emergence across the different concentrations was similar, at close to 100% (Figure 28). Transgenic plants were then selected to germinate in the presence of 0–50 µM KCN since 50 µM was the concentration to be used for the root elongation assays. KCN did not affect the emergence of the radicle from the seed coat in transgenic plants either (Figure 29).

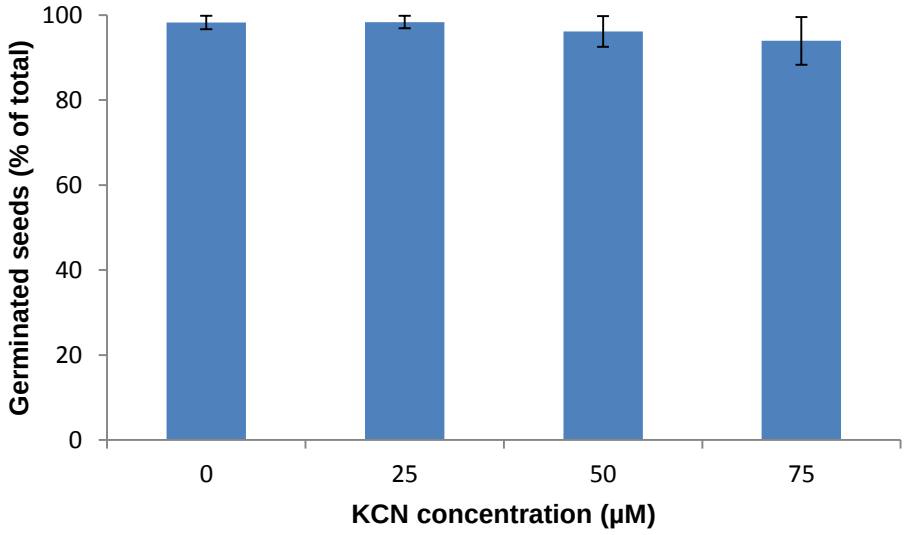

Figure 28: Wild-type *A. thaliana* Col-0 seeds germinate in the presence of CN. The mean germination rate (*n* = 3) of seeds sown directly onto KCN-containing media and incubated for two days is shown. Each replicate contained 40 seeds. Error bars indicate standard deviation.

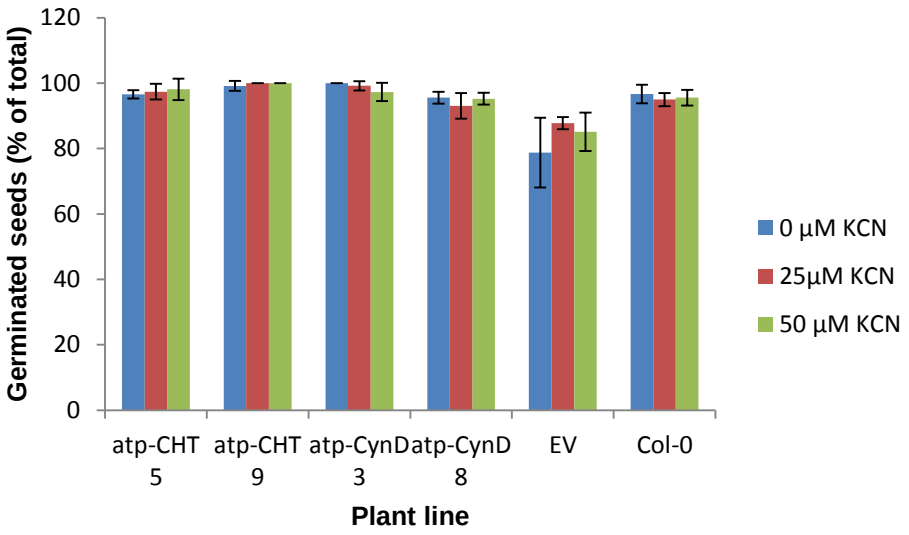

Figure 29: Transgenic *A. thaliana* seeds germinate in the presence of CN. The mean germination rate (*n* = 3) of transgenic seeds sown directly onto KCN-containing media and incubated for two days is shown. Each replicate contained 40 seeds. Error bars represent standard deviation. EV: empty vector control; Col-0: wild-type control.

Root elongation assays of transgenic *A. thaliana* germinated on cyanide

Having determined that the germination of transgenic seeds was also unaffected by CN, a root elongation assay to determine whether the transgenic plants could tolerate CN in the growth media was performed. Based on the qPCR expression data and the initial root elongation assays, two lines with the highest transgene expression were selected from *atp-CHT* and *atp-CynD* plant lines for CN tolerance analysis: *atp-CHT* 7 and 10; and *atp-CynD* 1 and 3. T_3 seeds were stratified and sown directly onto 50 mL of half-strength MS agar with either 62.5 µL 40mM KCN (in 25mM KOH), giving a final KCN concentration of 50 µM, or 62.5 µL of 25 mM KOH. The latter served as a control to demonstrate that any differences in root growth were due to the presence of KCN rather than change in media pH due to KOH. 50 µM KCN was chosen because this concentration caused an approximately 50% reduction in initial root elongation experiments (Figure 27). Seven days after plating, the average new growth of tap roots exposed to 50 µM KCN as a proportion of the average new growth on media containing KOH (relative mean) for each line was compared (Figure 30).

While all the plant lines tested displayed reduced growth on CN compared to control media, the transgenic plants showed increased CN tolerance compared to wild-type Col-0. In keeping with the initial root elongation experiment (Figure 27), Col-0 growth was reduced by approximately 50% upon exposure to 50 µM KCN in the growth media. Importantly, EV plants displayed the same growth as wild-type, indicating that any difference in transgenic plant growth was due to the transgene. *atp-*

CynD 1 and *atp-CynD* 3, both with relative root growth of approximately 75%, displayed the best CN tolerance compared to Col-0. *atp-CHT* 7 and *atp-CHT* 10 had growth at 70% of that in normal media. There was no statistically significant difference between the transgenic lines. These results suggest that the enhanced tolerance may have been due to translation of the expressed transgenes into functional proteins, enabling detoxification of more CN than occurred in Col-0.

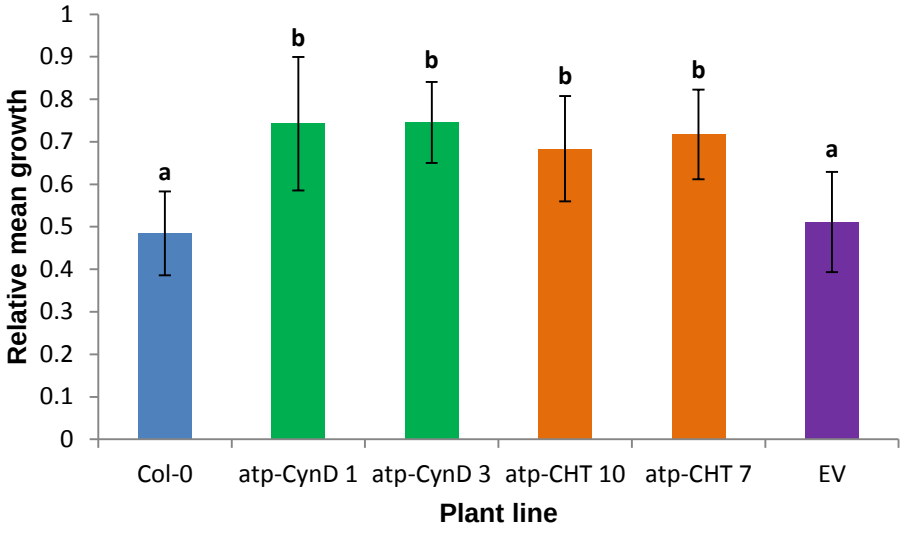

Figure 30: Root length of seven-day-old transgenic *A. thaliana* plant lines germinated on 50 µM KCN relative to the average growth of the same genotype in the absence of KCN. A) Seeds were sown onto media with and without KCN and grown for seven days. The tap root growth on CN (*n* = 14–18) was normalized to the mean of that in the absence of CN (KOH only) for each plant line (*n* = 15–19) to obtain the relative root growth in the presence of CN. Relative mean growth values labelled with different letters are significantly different from wild-type ($P < 0.01$, Student's *t*-test). Error bars represent standard deviation. EV: empty vector control; Col-0: wild-type control. Results shown are from one experiment representative of two.

Higher relative expression of the same transgene did not lead to increased CN tolerance for plants. *atp-CynD* 3 and *atp-CHT* 10 had the highest relative expression of their respective transgene (Figures 24 and 25). The relative expression level in *atp-CynD* 1 plants was 30% less than that in *atp-CynD* 3 (Figure 25) but there was no significant difference in growth on CN between the two lines. Similarly, a 20% difference in expression between *atp-CHT* 7 and *atp-CHT* 10 (Figure 24) lines did not result in a significant difference in growth. A possible explanation for this may be that expression above a threshold level for each transgene is sufficient to confer increased CN tolerance on plants. Transcript levels do not necessarily correlate directly with protein abundance (Vogel & Marcotte, 2012) therefore conclusions about enzyme activity and the degree of CN tolerance of one plant line relative to other tolerant transgenic lines cannot be made on the basis of transgene expression.

Future work with these transgenic plants could include assaying enzyme activity within the different plant lines to establish whether it correlates with CN tolerance.

The current study demonstrated that *B. pumilus CynD* and *N. crassa CHT* could be heterologously expressed in transgenic *A. thaliana* Col-0. Further, mitochondrial-targeted expression of the encoded enzymes was shown to enhance CN tolerance in *A. thaliana*. It is interesting to note that the improvements in plant growth on CN observed in this study were similar to those achieved in other recently published studies. In their experiments, Kebeish et al. (2015) reported a 56% increase in tap root growth compared to control plants for Arabidopsis over-expressing endogenous FDH and the CynD from *Pseudomonas stutzeri* in chloroplasts. Previously, Arabidopsis expressing the pinA nitrilase from *Pseudomonas fluorescens* had shown tap root growth increase of approximately 35% compared to the wild-type (O'Leary, Preston & Sweetlove, 2014). The *CynD* and *CHT* transgenic lines studied here had a 41–54% root growth increase compared to the wild-type.

Although it was not confirmed that CynD and CHT were physically present in the mitochondria, the mitochondrial targeting *atp* presequence used has previously been shown to effectively target GFP to the mitochondria (Logan & Leaver, 2000). Notwithstanding that Kebeish et al. (2015) used a much higher CN concentration to test tolerance than O'Leary, Preston and Sweetlove (2014) and the present study, it is evident that targeting of transgenes to the different cellular compartments (chloroplast, mitochondria and cytosol) is effective for increasing Arabidopsis CN tolerance. In light of these results, a second attempt to generate plants expressing *CynD* and *CHT* in the cytosol that can be quantitated would be worthwhile. A comparison of the CN tolerance of these plants with *atp-CynD* and *atp-CHT* plants would be more instructive regarding the relationship between CN tolerance and site of expression, that is, whether there is a significant difference in CN tolerance between plants expressing these transgenes in the mitochondria compared to the cytosol.

By boosting the capacity for the removal of excess formate generated by the CynD reaction, by FDH, Kebeish et al. (2015) were able to increase CN tolerance compared to the wild-type control plants. The authors did not directly compare the *CynD* + *FDH* plants with *CynD* plants, therefore, it cannot be inferred what the effect of FDH expression was, exclusive of the effect of CynD expression, on CN tolerance. Therefore, FDH co-expression may or may not have the potential to improve CN tolerance in the plants expressing *B. pumilus CynD*.

Future work could include the generation of transgenic plants simultaneously expressing CN detoxification enzymes targeted to the cytoplasm, mitochondria and chloroplasts to determine whether there would be an additive effect on CN tolerance. To have potential utility in the phytoremediation of CN-contaminated soils, transformable plants with a greater biomass and higher innate CN detoxification capacity than Arabidopsis would have to be used.

CHAPTER 4: CONCLUSIONS

Phytoremediation has been identified as a relatively low-cost and environmentally friendly technology to use in addressing the problem of toxic concentrations of CN, from anthropogenic sources such as hydrometallurgical gold mining, in soil. The cyanide-degrading activity of plants is limited by the capacity of the endogenous CAS pathway for the detoxification of exogenous cyanide, such that the levels of CN found in the soil of contaminated sites are inhibitory to plant growth. Plants such as sorghum (Trapp et al., 2003) have demonstrated the potential for use in phytoremediation due to their high natural capacity for degradation of exogenous CN compared to other plants. Genetic engineering may provide a means by which limitations to CN detoxification could be overcome, allowing for the augmentation of the existing CAS pathway or the introduction of efficient synthetic CN detoxification pathways into plants.

The purpose of the present study was to determine whether heterologous expression of *B. pumilus* CynD and *N. crassa* CHT in *A. thaliana* would enhance its capacity for cyanide detoxification, thereby increasing cyanide tolerance. It was first established that the formate and formamide products of the CynD and CHT detoxification reactions were not likely to be harmful to transgenic plants because toxicity occurred at micromolar concentrations of CN compared to millimolar concentrations of formate and formamide. It was also established that CN in the growth media only had negative effects on the growth of seedlings and did not inhibit germination, as marked by radicle emergence from the seed coat, of wild-type and transgenic seeds. The results of this study showed that expression of either CynD or CHT in the mitochondria effectively increased the CN tolerance of *A. thaliana*. Tap root growth in the presence of CN, compared to on normal media, of plants expressing the gene encoding either protein was similar and significantly better than wild-type root growth. The 41–54% improvement on wild-type Col-0 root growth, of *atp-CynD* and *atp-CHT* plants in the presence of KCN, fell within the 35%–56% range of root length increase observed in previous studies which used microbial nitrilases to augment the CAS pathway in the cytoplasm (O'Leary, Preston & Sweetlove, 2014) and introduce a synthetic pathway to the chloroplasts (Kebeish et al., 2015). It is, however, important to note that although the root growth of transgenic plants was significantly greater than the wild-type in the presence of CN, it was still reduced compared to transgenic plants grown in the absence of CN. The present study was only the third known attempt at improving plant CN tolerance by genetic engineering. The challenge remains, therefore, to find a genetic strategy for increasing CN tolerance that allows normal plant growth in the presence of CN.

Another aim of this work was to determine whether targeting the enzymes to the mitochondria, where the inhibition of aerobic respiration by CN occurs, would result in greater CN tolerance than expression of the enzymes in the cytoplasm. A lack of detectable transgene expression in *CynD* plants, even though the transgene was integrated into the plant genome, meant that atp-CynD and CynD plants could not be compared. Similarly, *CHT* and atp-CHT plants could not be compared because the detected transgene expression in *CHT* plants could not be quantitated. A second attempt at generating plants expressing CHT and CynD in the cytoplasm, if successful, would allow the difference in cyanide tolerance to be quantified.

It is important that different genetic engineering strategies can increase CN tolerance as this means that a greater number of options are available when developing strategies for phytoremediation purposes. Simultaneously targeting the CAS pathway and introducing synthetic microbial pathways could be the next step in the development of plants for cyanide phytoremediation. A combination of the three strategies, that is, simultaneously augmenting the endogenous CAS pathway and introducing plastid-targeted synthetic CN degradation pathways from microorganisms could be assessed for any improvement in CN tolerance compared to the singular approaches previously attempted. For applicability in phytoremediation, the genetic engineering strategies identified as the most effective would have to be tested in plants which have a higher biomass and natural CN tolerance than Arabidopsis, and are amenable to transformation.

CHAPTER 5: REFERENCES

Akcil, A. 2003. Destruction of cyanide in gold mill effluents: biological versus chemical treatments. *Biotechnology Advances.* 21(6): 501-511.

Allen, J.F. & Whatley, F.R. 1978. Effects of inhibitors of catalase on photosynthesis and on catalase activity in unwashed preparations of intact chloroplasts. *Plant Physiology.* 61(6): 957-960.

Alström, S. & Burns, R.G. 1989. Cyanide production by rhizobacteria as a possible mechanism of plant growth inhibition. *Biology and Fertility of Soils.* 7(3): 232-238.

Basile, L., Willson, R., Sewell, B.T. & Benedik, M. 2008. Genome mining of cyanide-degrading nitrilases from filamentous fungi. *Applied Microbiology and Biotechnology.* 80(3): 427-435.

Bethke, P.C., Libourel, I.G.L. & Jones, R.L. 2006. Nitric oxide reduces seed dormancy in Arabidopsis. *Journal of Experimental Botany.* 57(3): 517-526.

Bethke, P.C., Libourel, I.G.L., Reinöhl, V. & Jones, R.L. 2006. Sodium nitroprusside, cyanide, nitrite, and nitrate break Arabidopsis seed dormancy in a nitric oxide-dependent manner. *Planta.* 223(4): 805-812.

Birke, H., Haas, F.H., De Kok, L.J., Balk, J., Wirtz, M. & Hell, R. 2012. Cysteine biosynthesis, in concert with a novel mechanism, contributes to sulfide detoxification in mitochondria of *Arabidopsis thaliana*. *Biochemical Journal.* 445: 275-283.

Blom, D., Fabbri, C., Eberl, L. & Weisskopf, L. 2011. Volatile-mediated killing of *Arabidopsis thaliana* by bacteria is mainly due to hydrogen cyanide. *Applied and Environmental Microbiology.* 77(3): 1000-1008.

Blumenthal, S.G., Hendrickson, H.R., Abrol, Y.P. & Conn, E.E. 1968. Cyanide metabolism in higher plants: III. The biosynthesis of β-cyanoalanine. *Journal of Biological Chemistry.* 243(20): 5302-5307.

Blumer, C. & Haas, D. 2000. Mechanism, regulation, and ecological role of bacterial cyanide biosynthesis. *Archives of Microbiology.* 173(3): 170-177.

Budde, M.W. & Roth, M.B. 2011. The response of *Caenorhabditis elegans* to hydrogen sulfide and hydrogen cyanide. *Genetics.* 189(2): 521-532.

Clough, S.J. & Bent, A.F. 1998. Floral dip: a simplified method for *Agrobacterium*-mediated transformation of *Arabidopsis thaliana*. *The Plant Journal.* 16(6): 735-743.

Dash, R.R., Gaur, A. & Balomajumder, C. 2009. Cyanide in industrial wastewaters and its removal: A review on biotreatment. *Journal of Hazardous Materials.* 163(1): 1-11.

Devi, K.K. & Kothamasi, D. 2009. *Pseudomonas fluorescens* CHA0 can kill subterranean termite *Odontotermes obesus* by inhibiting cytochrome *c* oxidase of the termite respiratory chain. *FEMS Microbiology Letters.* 300(2): 195-200.

Ebbs, S. 2004. Biological degradation of cyanide compounds. *Current Opinion in Biotechnology.* 15(3): 231-236.

Ebbs, S.D., Kosma, D.K., Nielson, E.H., Machingura, M., Baker, A.J.M. & Woodrow, I.E. 2010. Nitrogen supply and cyanide concentration influence the enrichment of nitrogen from cyanide in wheat (*Triticum aestivum L.*) and sorghum (*Sorghum bicolor L.*). *Plant, Cell & Environment.* 33(7): 1152-1160.

Edwards, K., Johnstone, C. & Thompson, C. 1991. A simple and rapid method for the preparation of plant genomic DNA for PCR analysis. *Nucleic Acids Research.* 19(6): 1349.

Eisler, R. & Wiemeyer, S. 2004. Cyanide hazards to plants and animals from gold mining and related water issues. *Reviews of Environmental Contamination and Toxicology.* 183:21-54.

Eliceiri, K.W., Rasband, W.S. & Schneider, C.A. 2012. NIH Image to ImageJ: 25 years of image analysis. *Nature Methods.* 9(7):671-675.

Elthon, T.E., Nickels, R.L. & McIntosh, L. 1989. Monoclonal antibodies to the alternative oxidase of higher plant mitochondria. *Plant Physiology.* 89(4): 1311-1317.

Flematti, G.R., Merritt, D.J., Piggott, M.J., Trengove, R.D., Smith, S.M., Dixon, K.W. & Ghisalberti, E.L. 2011. Burning vegetation produces cyanohydrins that liberate cyanide and stimulate seed germination. *Nature Communications.* 2:360.

Fokunang, C.N., Tomkins, P.T., Dixon, A.G.O., Tembe, E.A, Salwa, B., Nukenine, E.N. & Horan, I. 2001. Cyanogenic potential in food crops and its implication in cassava (*Manihot esculenta* Crantz) Production. *Pakistan Journal of Biological Sciences.* 4(7):926-930.

Forti, G. & Gerola, P. 1977. Inhibition of photosynthesis by azide and cyanide and the role of oxygen in photosynthesis. *Plant Physiology.* 59(5): 859-862.

García, I., Castellano, J.M., Vioque, B., Solano, R., Gotor, C. & Romero, L.C. 2010. Mitochondrial β-cyanoalanine synthase is essential for root hair formation in *Arabidopsis thaliana*. *The Plant Cell Online.* 22(10): 3268-3279.

Gasteiger, E., Gattiker, A., Hoogland, C., Ivanyi, I., Appel, R.D. & Bairoch, A. 2003. ExPASy: the proteomics server for in-depth protein knowledge and analysis. *Nucleic Acids Research.* 31(13): 3784-3788.

Gibeaut, D.M., Hulett, J., Cramer, G.R. & Seemann, J.R. 1997. Maximal biomass of *Arabidopsis thaliana* using a simple, low-maintenance hydroponic method and favorable environmental conditions. *Plant Physiology.* 115(2): 317-319.

Goudey, J.S., Tittle, F.L. & Spencer, M.S. 1989. A role for ethylene in the metabolism of cyanide by higher plants. *Plant Physiology.* 89(4): 1306-1310.

Hatzfeld, Y., Maruyama, A., Schmidt, A., Noji, M., Ishizawa, K. & Saito, K. 2000. β-cyanoalanine synthase is a mitochondrial cysteine synthase-like protein in spinach and Arabidopsis. *Plant Physiology.* 123(3): 1163-1172.

Holsters, M., Silva, B., Van Vliet, F., Genetello, C., De Block, M., Dhaese, P., Depicker, A., Inzé, D. et al. 1980. The functional organization of the nopaline *A. tumefaciens* plasmid pTiC58. *Plasmid.* 3(2): 212-230.

Howden, A.J.M., Harrison, C.J. & Preston, G.M. 2009. A conserved mechanism for nitrile metabolism in bacteria and plants. *The Plant Journal.* 57(2): 243-253.

Ingvorsen, K., Højer-Pedersen, B. & Godtfredsen, S.E. 1991. Novel cyanide-hydrolyzing enzyme from *Alcaligenes xylosoxidans* subsp. *denitrificans*. *Applied and Environmental Microbiology.* 57(6): 1783-1789.

Jandhyala, D.M., Willson, R.C., Sewell, B.T. & Benedik, M.J. 2005. Comparison of cyanide-degrading nitrilases. *Applied Microbiology and Biotechnology.* 68(3): 327-335.

John, P. 1997. Ethylene biosynthesis: The role of 1-aminocyclopropane-1-carboxylate (ACC) oxidase, and its possible evolutionary origin. *Physiologia Plantarum.* 100(3): 583-592.

Johnson, C.A (in press). The fate of cyanide in leach wastes at gold mines: An environmental perspective. *Applied Geochemistry.* DOI:http://dx.doi.org/10.1016/j.apgeochem.2014.05.023.

Jones, D.A. 1998. Why are so many food plants cyanogenic? *Phytochemistry.* 47(2): 155-162.

Kang, D., Hong, L.Y., Schwab, A.P. & Banks, M.K. 2008. Plant germination and growth after exposure to iron cyanide complexes. *Journal of Environmental Science and Health, Part A.* 43(6): 627-632.

Kebeish, R., Aboelmy, M., El-Naggar, A., El-Ayouty, Y. & Peterhansel, C. 2015. Simultaneous overexpression of cyanidase and formate dehydrogenase in *Arabidopsis thaliana* chloroplasts enhanced cyanide metabolism and cyanide tolerance. *Environmental and Experimental Botany.* 110: 19-26.

Knowles, C.J. 1976. Microorganisms and cyanide. *Bacteriological Reviews.* 40(3): 652-680.

Kojima, M., Poulton, J.E., Thayer, S.S. & Conn, E.E. 1979. Tissue distributions of dhurrin and of enzymes involved in its metabolism in leaves of S*orghum bicolor*. *Plant Physiology.* 63(6): 1022-1028.

Korte, F., Spiteller, M. & Coulston, F. 2000. The cyanide leaching gold recovery process is a nonsustainable technology with unacceptable impacts on ecosystems and humans: The disaster in Romania. *Ecotoxicology and Environmental Safety.* 46(3): 241-245.

Larsen, M., Trapp, S. & Pirandello, A. 2004. Removal of cyanide by woody plants. *Chemosphere.* 54(3): 325-333.

Liang, W. 2003. Drought stress increases both cyanogenesis and β-cyanoalanine synthase activity in tobacco. *Plant Science.* 165(5): 1109-1115.

Life Technologies. 2014. Real-Time PCR: Understanding C_t Application Note. Available: www.lifetechnologies.com/za/en/home/life-science/pcr/real-time-pcr/qpcr-education/pcr-understanding-ct-application-note.html[2014, October 31]

Logan, D.C. & Leaver, C.J. 2000. Mitochondria-targeted GFP highlights the heterogeneity of mitochondrial shape, size and movement within living plant cells. *Journal of Experimental Botany.* 51(346): 865-871.

Machingura, M. & Ebbs, S.D. 2010. Increased β-cyanoalanine synthase and asparaginase activity in nitrogen-deprived wheat exposed to cyanide. *Journal of Plant Nutrition and Soil Science.* 173(6): 808-810.

Machingura, M. & Ebbs, S.D. 2014. Functional redundancies in cyanide tolerance provided by β-cyanoalanine pathway genes in *Arabidopsis thaliana*. *International Journal of Plant Sciences.* 175(3): 346-358.

McMahon Smith, J. & Arteca, R.N. 2000. Molecular control of ethylene production by cyanide in *Arabidopsis thaliana*. *Physiologia Plantarum.* 109(2): 180-187.

Meyer, T., Burow, M., Bauer, M. & Papenbrock, J. 2003. Arabidopsis sulfurtransferases: investigation of their function during senescence and in cyanide detoxification. *Planta.* 217(1): 1-10.

Meyers, P.R., Rawlings, D.E., Woods, D.R. & Lindsey, G.G. 1993. Isolation and characterization of a cyanide dihydratase from *Bacillus pumilus* C1. *Journal of Bacteriology.* 175(19): 6105-6112.

Meyers, P.R., Gokool, P., Rawlings, D.E. & Woods, D.R. 1991. An efficient cyanide-degrading *Bacillus pumilus* strain. *Journal of General Microbiology.* 137(6): 1397-1400.

Miller, J.M. & Conn, E.E. 1980. Metabolism of hydrogen cyanide by higher plants. *Plant Physiology.* 65(6): 1199-1202.

Mudder, T.I. & Botz, M.M. 2004. Cyanide and society: a critical review. *European Journal of Mineral Processing & Environmental Protection.* 4(1): 62-74.

Murphy, L.J., Robertson, K.N., Harroun, S.G., Brosseau, C.L., Werner-Zwanziger, U., Moilanen, J., Tuononen, H.M. & Clyburne, J.A.C. 2014. A simple complex on the verge of breakdown: isolation of the elusive cyanoformate ion. *Science.* 344(6179): 75-78.

Nakamura, T., Yamaguchi, Y. & Sano, H. 2000. Plant mercaptopyruvate sulfurtransferases. *European Journal of Biochemistry.* 267(17): 5621.

Nelson, M.G., Kroegef, E.B. & Arps, P.J. 1998. Chemical and biological destruction of cyanide: comparative costs in a cold climate. *Mineral Processing and Extractive Metallurgy Review.* 19(1): 217-226.

O'Leary, B., Preston, G.M. & Sweetlove, L.J. 2014. Increased β-cyanoalanine nitrilase activity improves cyanide tolerance and assimilation in Arabidopsis. *Molecular Plant.* 7(1): 231-243.

Oracz, K., El-Maarouf-Bouteau, H., Kranner, I., Bogatek, R., Corbineau, F. & Bailly, C. 2009. The mechanisms involved in seed dormancy alleviation by hydrogen cyanide unravel the role of reactive oxygen species as key factors of cellular signaling during germination. *Plant Physiology.* 150(1): 494-505.

Peiser, G.D., Wang, T., Hoffman, N.E., Yang, S.F., Liu, H. & Walsh, C.T. 1984. Formation of cyanide from carbon 1 of 1-aminocyclopropane-1-carboxylic acid during its conversion to ethylene. *Proceedings of the National Academy of Sciences.* 81(10): 3059-3063.

Pilon-Smits, E. 2005. Phytoremediation. *Annual Review of Plant Biology.* 56(1): 15-39.

Piotrowski, M., Schönfelder, S. & Weiler, E.W. 2001. The *Arabidopsis thaliana* isogene NIT4 and its orthologs in tobacco encode β-cyano-l-alanine hydratase/nitrilase. *Journal of Biological Chemistry.* 276(4): 2616-2621.

Piotrowski, M. & Volmer, J. 2006. Cyanide metabolism in higher plants: cyanoalanine hydratase is a NIT4 homolog. *Plant Molecular Biology.* 61(1-2): 111-122.

Poulton, J.E. 1990. Cyanogenesis in Plants. *Plant Physiology.* 94(2): 401-405.

Prabhu, V., Chatson, K.B., Abrams, G.D. & King, J. 1996. ^{13}C nuclear magnetic resonance detection of interactions of serine hydroxymethyltransferase with C1-tetrahydrofolate synthase and glycine decarboxylase complex activities in Arabidopsis. *Plant Physiology.* 112(1): 207-216.

Romero, L.C., Aroca, M.Á, Laureano-Marín, A.M., Moreno, I., García, I. & Gotor, C. 2014. Cysteine and cysteine-related signaling pathways in *Arabidopsis thaliana*. *Molecular Plant.* 7(2): 264-276.

Schenk, P.M., Kazan, K., Manners, J.M., Anderson, J.P., Simpson, R.S., Wilson, I.W., Somerville, S.C. & Maclean, D.J. 2003. Systemic gene expression in Arabidopsis during an incompatible interaction with A*lternaria brassicicola*. *Plant Physiology.* 132(2): 999-1010.

Shimada, T.L., Shimada, T. & Hara-Nishimura, I. 2010. A rapid and non-destructive screenable marker, FAST, for identifying transformed seeds of *Arabidopsis thaliana*. *The Plant Journal.* 61(3): 519-528.

Shiraishi, T., Fukusaki, E. & Kobayashi, A. 2000. Formate dehydrogenase in rice plant: Growth stimulation effect of formate in rice plant. *Journal of Bioscience and Bioengineering.* 89(3): 241-246.

Skowronski, B. & Strobel, G.A. 1969. Cyanide resistance and cyanide utilization by a strain of *Bacillus pumilus*. *Canadian Journal of Microbiology.* 15(1): 93-98.

Taylorson, R.B. & Hendricks, S.B. 1973. Promotion of seed germination by cyanide. *Plant Physiology.* 52(1): 23-27.

Thayer, S.S. & Conn, E.E. 1981. Subcellular localization of dhurrin ß-glucosidase and hydroxynitrile lyase in the mesophyll cells of *Sorghum* leaf blades. *Plant Physiology.* 67(4): 617-622.

Trapp, S., Larsen, M., Pirandello, A. & Danquah-Boakye, J. 2003. Feasibility of cyanide elimination using plants. *European Journal of Mineral Processing & Environmental Protection.* 3(1): 128-137.

Vetter, J. 2000. Plant cyanogenic glycosides. *Toxicon.* 38(1): 11-36.

Vogel, C. & Marcotte, E.M. 2012. Insights into the regulation of protein abundance from proteomic and transcriptomic analyses. *Nature Reviews.Genetics.* 13(4): 227-232.

Watanabe, M., Kusano, M., Oikawa, A., Fukushima, A., Noji, M. & Saito, K. 2008. Physiological roles of the β-substituted alanine synthase gene family in Arabidopsis. *Plant Physiology.* 146(1): 310-320.

Way, J.L. 1984. Cyanide intoxication and its mechanism of antagonism. *Annual Review of Pharmacology and Toxicology.* 24(1): 451-481.

Weigel, D. & Glazebrook, J. 2002. *Arabidopsis: A Laboratory Manual*. Cold Spring Harbor Laboratory Press, Cold Spring Harbor, New York.

Wen, J., Huang, F., Liang, W. & Liang, H. 1997. Increase of HCN and β-cyanoalanine synthase activity during ageing of potato tuber slices. *Plant Science.* 125(2): 147-151.

Wingler, A., Lea, P.,J. & Leegood, R.,C. 1999. Photorespiratory metabolism of glyoxylate and formate in glycine-accumulating mutants of barley and *Amaranthus edulis*. *Planta.* 207(4): 518-526.

Wishnick, M. & Lane, M.D. 1969. Inhibition of ribulose diphosphate carboxylase by cyanide: inactive ternary complex of enzyme, ribulose diphosphate, and cyanide. *Journal of Biological Chemistry.* 244(1): 55-59.

Yip, W. & Yang, S.F. 1988. Cyanide metabolism in relation to ethylene production in plant tissues. *Plant Physiology.* 88(2): 473-476.

Yu, X., Gu, J. & Liu, S. 2007. Biotransformation and metabolic response of cyanide in weeping willows. *Journal of Hazardous Materials.* 147(3): 838-844.

Yu, X., Lu, P. & Yu, Z. 2012. On the role of β-cyanoalanine synthase (CAS) in metabolism of free cyanide and ferri-cyanide by rice seedlings. *Ecotoxicology.* 21(2): 548-556.

Yu, X., Trapp, S., Zhou, P. & Hu, H. 2005. The effect of temperature on the rate of cyanide metabolism of two woody plants. *Chemosphere.* 59(8): 1099-1104.

Yu, X., Trapp, S., Zhou, P., Wang, C. & Zhou, X. 2004. Metabolism of cyanide by Chinese vegetation. *Chemosphere.* 56(2): 121-126.

Zagrobelny, M., Bak, S., Rasmussen, A.V., Jørgensen, B., Naumann, C.M. & Lindberg Møller, B. 2004. Cyanogenic glucosides and plant–insect interactions. *Phytochemistry.* 65(3): 293-306.

Zagury, G.J., Oudjehani, K. & Deschênes, L. 2004. Characterization and availability of cyanide in solid mine tailings from gold extraction plants. *Science of the Total Environment.* 320(2–3): 211-224.